UCRL-17731

cy. 2

University of California

Ernest O. Lawrence Radiation Laboratory

INADEQUACY OF THE SIMPLE DWBA TREATMENT OF COMPARATIVE (p, t) AND (p, ^{3}He) TRANSITIONS

Donald G. Fleming, Joseph Cerny, and Norman K. Glendenning

July 1967

Berkeley, California

Submitted to the Physical Review
Sections 51.6, 53.5

UCRL-17731
Preprint

UNIVERSITY OF CALIFORNIA

Lawrence Radiation Laboratory and
Department of Chemistry
Berkeley, California

AEC Contract No. W-7405-eng-48

INADEQUACY OF THE SIMPLE DWBA TREATMENT OF COMPARATIVE (p,t) AND (p,^{3}He) TRANSITIONS

Donald G. Fleming, Joseph Cerny, and Norman K. Glendenning

July 1967

INADEQUACY OF THE SIMPLE DWBA TREATMENT OF COMPARATIVE (p,t) AND (p,^{3}He) TRANSITIONS*

UCRL-17731

Donald G. Fleming,† Joseph Cerny, and Norman K. Glendenning
Department of Chemistry and
Lawrence Radiation Laboratory
University of California
Berkeley, California

ABSTRACT

Current theories of direct two-nucleon transfer reactions are tested by comparing (p,t) and (p,^{3}He) transitions on odd mass nuclei leading to mirror final states. Proton induced reactions on ^{15}N at 43.7 MeV and on ^{13}C at 49.6 MeV are discussed in detail. Many mirror transitions are analyzed with DWBA calculations in an attempt to fit both angular distributions and cross-section ratios; good results for the shapes of the angular distributions are obtained. The agreement between theory and experiment for the cross-section ratios of mirror (p,t) to (p,^{3}He) transitions improves in every case with the inclusion of a strongly spin-dependent force in the nucleon-nucleon interaction, but overall satisfactory agreement is not obtained. The (p,t) transitions are found to be generally stronger than expected, relative to their mirror (p,^{3}He) transitions, and three cases are discussed where the experimental ratios of these cross sections exceed the theoretical upper limit. Two possibilities, both of which introduce coherent effects, are discussed to account for this result: 1) interference terms arising through a spin-orbit interaction in the optical potential or 2) interference terms between a direct reaction contribution and a core-excitation contribution to the cross section.

---

*Work performed under the auspices of the U.S. Atomic Energy Commission.

†Now at the Nuclear Structure Laboratory, University of Rochester, Rochester, New York.

I. INTRODUCTION

Earlier work has shown the utility of comparative (p,t) and (p,^{3}He) transitions in investigating the charge independence of nuclear forces (1) and in identifying states of high isospin—in particular, T=3/2 (2) and T=2 (3) levels. In addition, however, similar comparative measurements of these reactions on odd mass (T=1/2) targets populating mirror final states provide one with a sensitive test of some of the assumptions made in current theories of direct two-nucleon transfer reactions.[4,5]

Of particular interest in such (p,t) vs (p,^{3}He) comparisons is an understanding of the influence of the greater flexibility of the (p,^{3}He) reaction, which in first order permits a ^{31}S and ^{13}S spin-isospin transfer of a neutron-proton pair, as compared to the (p,t) reaction, which only allows a ^{13}S transfer of two neutrons. The population of mirror final states permits such comparisons with minimal uncertainty in the final state wave functions. In most previously reported work,[1-3] such comparisons were not discussed because final states of high isospin were of interest, and hence a pure ^{13}S transfer of both nucleon pairs was required.

In general, it is found that (p,t) cross sections to mirror final states—when not inhibited by nuclear structure considerations—are strongly enhanced over the corresponding (p,^{3}He) transitions, sometimes by factors as large as four or five, and we will consider the implications of this enhancement in some detail. The only previous work discussing (p,t) and (p,^{3}He) transitions to mirror final states has been by Cerny et al.,[6] who recently

studied the mass 5 and mass 7 final nuclei by comparing these reactions on targets of ^{7}Li and ^{9}Be, respectively. Although the (p,t) transitions reported in Ref. 6 were generally found to be stronger than their corresponding mirror (p,^{3}He) transitions, these reactions also show striking examples of the influence of nuclear structure in inhibiting certain (p,t) transitions. This current exploration of comparative (p,t) and (p,^{3}He) reactions will examine in detail the three target nuclei ^{15}N, ^{13}C, and ^{31}P leading to mirror final states in the mass 13, 11, and 29 nuclei, respectively.

II. THEORY

The theory of direct two-nucleon transfer reactions was developed beyond earlier plane wave treatments almost simultaneously by a number of authors,[4,5] although the formulation of Ref. (4) will be used throughout this work. The reader is referred to Ref. (4) for a more detailed discussion of the theory than is presented below.

Assuming that spin-orbit coupling can be neglected in the entrance and exit channels, the differential cross section of a two-nucleon transfer reaction can be written as an incoherent sum over the angular momentum quantum numbers (L, S, J, T) of the transferred pair:

$$\frac{d\sigma}{d\Omega} \propto \sum_{LSJT} C_{ST}^{2} \sum_{M} \left| \sum_{N} G_{NLSJT} B_{NL}^{M} \right|^{2} \qquad (1)$$

The G_{NLSJT} factor arises from an overlap integral between the initial and final nuclear states and—like the single nucleon transfer spectroscopic factor—contains the nuclear structure information. It is designated throughout this paper as the nuclear structure factor. However, unlike a single nucleon transfer reaction where the spectroscopic factor is merely multiplicative, the G's are involved coherently in the transition amplitude of a two-nucleon transfer reaction and therefore cannot be extracted from the experimental data.[4] Instead, they must be calculated from assumed nuclear wave functions and tested for consistency with experiment. Agreement between theory and experiment can then be used as a sensitive test of the wave functions describing the initial and final nuclear states, and several calculations of this kind have recently been reported.[7-9]

The factor B_{NL}^{M} is the usual distorted wave amplitude, which is evaluated in zero range approximation and which contains the bound state wave function for the center-of-mass state (NL) of the transferred pair. The bound state wave function is represented by a harmonic oscillator in the nuclear interior and is matched at the nuclear surface to a Hankel function tail (which is characterized by the separation energy of the pair). The optical potential is assumed to be a central interaction with no spin-orbit potential; Saxon-Wood form factors are used throughout.

The factor C_{ST}^{2} is a spin-isospin coupling factor and, for a pickup reaction, is defined as—

$$C_{ST}^{2} = b_{ST}^{2} \left| \langle t_f m_f T M_T | t_i m_i \rangle \right|^2 \qquad (2)$$

where the Clebsch-Gordon coefficient involves the heavy nuclei in the reaction and couples the isospin of the initial and final states by the isospin (T) of the transferred pair. If the neutron-proton scheme is used in constructing the nuclear structure factors, then this coefficient is not applicable. The factor b_{ST}^2 is a spectroscopic overlap integral involving the light particles in the reaction,[4] which when generalized to include a spin-dependent nucleon-nucleon interaction, takes the form

$$b_{ST}^2 = \begin{cases} a_0^2(\delta_{S0}\,\delta_{T1}) & (p,t) \\ 1/2\left[a_0^2(\delta_{S0}\,\delta_{T1}) + a_1^2\,(\delta_{S1}\,\delta_{T0})\right] & (p,{}^3\mathrm{He}) \end{cases} \qquad (3)$$

where a_0^2 and a_1^2 arise from the spin exchange properties of the two-nucleon force, as described below. Under the usual simplification of a pure $^2S_{1/2}$ configuration for the triton or helium-3 wave function, only relative $\ell=0$ states of motion are allowed in the transfer of two nucleons (calculations on the amount of $^2S_{1/2}$ expected in the $A=3$ ground-state wave function range upward from 94%).[10] Assuming a pure $^2S_{1/2}$ state, the Pauli Principle restricts the (p,t) reaction to pure ^13S spin-isospin transfers but does not so restrict the $(p,{}^3\mathrm{He})$ reaction, ^13S and ^31S transfers both being allowed.

Expression (3) arises from an overlap integral involving the spin-isospin wave functions of the transferred pair and the $A=3$ ground-state wave function. Transfer of the pair in the spin state S involves the matrix element—

$$\langle \chi^{\sigma_b\ \tau_b}_{1/2\ 1/2}(1,2,3) \left| V_{13}(r_{13})+V_{23}(r_{23}) \right| \chi^{\sigma_a\ \tau_a}_{1/2\ 1/2}(3) \chi^{M_S\ M_T}_{S\ T}(1,2) \rangle \tag{4}$$

$$\equiv \langle 1/2\ \sigma_a\ S\ M_s \,|\, 1/2\ \sigma_b \rangle \sqrt{2S+1}\ b_{ST}$$

where, in our case, channel a represents the incident proton (with spin, isospin projections σ_a, τ_a) and channel b represents the outgoing triton or helium-3. The transferred pair is represented by the wave function χ_{ST} with projection quantum numbers M_S and M_T. V_{ij} is the two-body interaction between the incident proton (particle 3) and either one of the nucleons (particles 1,2) in the transferred pair, which in general may be transferred in either an S=0, T=1 state (^{13}S) or an S=1, T=0 state (^{31}S). We represent the singlet-even strength of the two-body potential V_{ij} by A^S and the triplet-even strength by A^T. Then the dependence of the matrix element (4) on these parameters for transfer of the pair in singlet or triplet spin states is given, respectively, by:

$$a_0 = 3/4\ A^T + 1/4\ A^S \tag{5a}$$

$$-a_1 = 1/4\ A^T + 3/4\ A^S \tag{5b}$$

For the (p,t) reaction, only the $a_0(S=0)$ term will contribute; for the (p,^{3}He) reaction, however, both the $a_0(S=0)$ and $a_1(S=1)$ terms are important. Writing Eq. (4) in terms of a_0 and a_1, and expressing the overlap in terms of a fractional parentage expansion (which introduces a factor of 1/2) and performing an incoherent sum of squares, as required by the assumption of a zero spin-orbit interaction in the optical model, yield the result given in Eq. (3).

The intrinsic ratio of a_0^2 to a_1^2 depends upon the nature of the nucleon-nucleon force. Evidence that the tensor force influences nucleon-nucleon scattering,[11] as well as evidence from model-dependent central-force calculations of S-wave scattering[12] and the bound state of the deuteron, lead us to expect some spin dependence in these pickup reactions. Moreover, a variety of shell model calculations indicate that the tensor force is strong[13,14] and that the ratio of the singlet-even (A^S) strength to the triplet-even (A^T) strength should be about 0.6/1.[13, 15] As we shall see, the data suggest use of a more strongly spin-dependent interaction than this, and we choose $A^S = 0.3\,A^T$. If the nucleon-nucleon interaction were spin-independent, then $A^S = A^T$ and $a_0^2/a_1^2 = 1.0$, so that there would be equal probability of transferring two nucleons in either S=0 or S=1 spin states in the $(p,{}^3He)$ reaction. However, this is no longer true for the case of a spin-dependent interaction and for our particular choice, $a_0^2/a_1^2 = 3.0$, so that for a given final state, the S=0 transfer is enhanced by a factor of three over the S=1 transfer.

In comparing (p,t) and $(p,{}^3He)$ reactions to mirror final states, it is instructive to calculate the theoretical cross section ratio expected for these transitions based on the limit of a pure S=0 transfer for the $(p,{}^3He)$ reaction:

$$\left.\frac{\sigma(p,t)}{\sigma(p,{}^3He)}\right\}_{S=0} = \frac{C_{ST}^2(p,t)}{C_{ST}^2(p,{}^3He)} \cdot \frac{\sum_{J\,M} \left|\sum_N G_{NJT}\, B_{NL}^M\right|^2}{\sum_{J\,M} \left|\sum_N G_{NJT}\, B_{NL}^M\right|^2} \qquad (6)$$

Experimental results for (p,t) and $(p,{}^3He)$ transitions from T=1/2 initial states to T=3/2 final states—where only a zero spin transfer is allowed—

show that the second ratio is essentially unity (within 10%). Both in the 1p shell[2] and in the 2s1d shell[16,17] these transitions to analog T=3/2 final states are found to be virtually identical.[18,19] Therefore Eq. (6) becomes

$$\left.\frac{\sigma(p,t)}{\sigma(p,{}^3He)}\right\}_{S=0} = \frac{C_{ST}{}^2(p,t)}{C_{ST}{}^2(p,{}^3He)} = \frac{1\cdot|\langle \tfrac{1}{2}-\tfrac{1}{2}\,1\;1|\tfrac{1}{2}\;\tfrac{1}{2}\rangle|^2}{\tfrac{1}{2}\cdot|\langle \tfrac{1}{2}\;\tfrac{1}{2}\,1\;0|\tfrac{1}{2}\;\tfrac{1}{2}\rangle|^2} = \frac{4}{1} \qquad (7)$$

On the basis of the earlier assumptions, then, this represents the upper bound that can be expected in comparing (p,t) and (p,^{3}He) cross sections,[20] since an incoherent contribution of S=1 transfer in the (p,^{3}He) reaction could only reduce this ratio.

III. RESULTS AND DISCUSSION

The two-nucleon transfer theory under discussion[4] has been successfully tested on targets of widely varying mass. Mangelson and Harvey[7] have obtained good fits to the angular distributions found in the $^{12}C(^3He,p)^{14}N$ reaction and Glendenning[8] has had equally good results in fitting the $^{208}Pb(p,t)^{206}Pb$ reaction. Since the (p,t) angular distributions to be presented below are also well predicted, we will assume that the theory properly takes into account the dynamics of the direct two-nucleon transfer reaction.

Of particular concern is the ability of the theory to fit the shapes and the magnitudes of the (p,^{3}He) transitions relative to the (p,t) transitions. Although this will depend somewhat on the choice of acceptable optical model parameters, the theoretical ratios of (p,t) to (p,^{3}He) cross sections

should be relatively insensitive to this choice. We will thus seek an explanation for the experimental ratios of (p,t) to (p,^{3}He) cross sections in terms of the theory based on a spin-independent nucleon-nucleon interaction ($A^S = A^T$) as well as the case of a strongly spin-dependent interaction ($A^S = 0.3\ A^T$). The introduction of this spin-dependent force will alter the relative (p,t) and (p,^{3}He) cross sections and hence alter the ratios to be compared; in addition, it may also change the shapes of those (p,^{3}He) angular distributions in which multiple L values are allowed.

Finally, we attempt to understand the general implication of the few observed experimental transitions in which the ratio of the (p,t) to the (p,^{3}He) cross sections are above the upper limit of 4/1 predicted by the theory.

A. $^{15}N(p,t)^{13}N$ and $^{15}N(p,^3He)^{13}C$

These reactions were induced by a 43.7-MeV proton beam from the Berkeley 88" cyclotron. Complete experimental results and their discussion are presented in a following paper.[21] Here only a few strong transitions are considered in order to test the assumptions of the theory. Figure 1 presents energy spectra taken at 22 degrees in the laboratory. The levels of interest are the strong states populated in the two reactions, ranging in excitation from 0 to 8 MeV; they are listed in Table I, along with their major configurations predicted from intermediate coupling wave functions.[22] Figures 2 through 4 compare angular distributions with distorted wave Born approximation (DWBA) calculations. Error bars, where shown, reflect only statistical uncertainties. Each theoretical fit is arbitrarily normalized at some forward

angle to the data and the (p,t) and (p,^{3}He) transitions are normalized independently of each other. Two-nucleon structure factors were calculated from coefficients of fractional parentage provided by Kurath[22] and as such are calculated on the basis of a complete intermediate coupling wave function for these mass 13 final states. General formulas used in the calculation of two-nucleon parentage factors for these reactions are given in Ref. 21 and the choice of optical model potentials used in fitting the data is also discussed in this reference. The optical potentials used are presented in Table II, along with those used in the ^{13}C and ^{31}P calculations to be discussed below. The same optical potential was used for both tritons and helium-3 in the exit channel.

Although the (p,t) ground state transition (L=0) shown in Fig. 2 is over-predicted by the theory at back angles, the general structure is quite well reproduced. Furthermore the 3.51 MeV ($3/2^-$) and 7.38 MeV ($5/2^-$) transitions (both L=2) shown in Figs. 3 and 4, respectively, are well predicted by the theory. In addition, the fits to the (p,^{3}He) angular distributions shown in Figs. 2 through 4, which assume a spin-independent nucleon-nucleon interaction, are fairly good. The effect of introducing a spin-dependent interaction is to alter the relative amounts of L=0 and L=2 in these (p,^{3}He) transitions, since the factor C_{ST}^2 in the differential cross section of Eq. (1) will be altered. The particular choice made ($A^S = 0.3\ A^T$) strongly enhances the S=0 transfer, resulting in a considerable increase of the L=0 component in the ground state transition but causing little difference in the 3.68 MeV transition. The effect of this is shown in Fig. 5, which presents normalized (p,^{3}He) fits to the ground state ($1/2^-$) and 3.68 MeV ($3/2^-$) transitions, utilizing the spin-dependent interaction. The ground state transition is now better fit

by the theory, while the $3/2^-$ transition shows no significant change. Although the optical model parameters used in this study were obtained by interpolation from parameters given in the literature for neighboring nuclei, and as such are certainly subject to inaccuracies, this effect of improving the ground state $(p,{}^3He)$ fit by introducing the spin-dependent force does reproduce for other choices of the helium-3 potential. The fit to the 7.55 MeV $(5/2^-)$ angular distribution shown in Fig. 4 is unaffected by a spin-dependent nucleon-nucleon interaction, since two-nucleon selection rules restrict this transition to a pure $L=2$ transfer.

Besides influencing the angular distributions of some $(p,{}^3He)$ transitions, a spin-dependent nucleon-nucleon force will also alter the relative cross sections for (p,t) and $(p,{}^3He)$ reactions. In particular, for the choice made of $A^S = 0.3\,A^T$, the (p,t) cross section and the $S=0$ component of the $(p,{}^3He)$ transition will be enhanced relative to the $S=1$ component of the $(p,{}^3He)$ transition. Before comparing any transitions, it is of interest to ascertain whether Coulomb and kinematic effects on the relative cross sections are important. For the reactions to be discussed in this and the following sections, the DWBA integrated cross sections for (p,t) and $(p,{}^3He)$ transitions to any given mirror pair, utilizing identical structure factors for both, were virtually the same.[23] Consequently, theory and experiment can be directly compared for each such pair.

Figure 6 presents a comparison of theoretical cross sections with experiment for the (p,t) and $(p,{}^3He)$ ground state transitions; the data are shown in $\mu b/sr$ and the theory is given in arbitrary units with no relative normalization. Two theoretical comparisons of these transitions are shown—one

for a spin-independent interaction and the other for the chosen spin-dependent interaction. Agreement between theory and experiment for the relative magnitudes of these transitions is certainly better in the case of the spin-dependent interaction. Similar comparisons have been made for the other levels discussed and the ratios (R) of their (p,t) to (p,^{3}He) integrated cross sections (the theory being integrated over the same range as the experiment) are presented in Table III. The overall result is that one has to invoke this strongly spin-dependent force in order to approach agreement between these theoretical ratios and the experimental ones. Noting the table, the $3/2^-$ level is relatively well predicted by our choice of a spin dependence while the ground state ($1/2^-$) transition is not. Nevertheless, the average agreement with experiment for these two levels is considerably improved. Of particular interest is the experimental ratio for the $5/2^-$ transition, which is greater than the limit of 4/1. Accordingly, the theoretical ratio for this transition is in the poorest agreement with experiment.

B. $^{13}C(p,t)^{11}C$ and $^{13}C(p,^3He)^{11}B$

This reaction was also studied at the Berkeley 88" cyclotron, with an incident proton energy of 49.6 MeV. Figure 7 presents energy spectra taken at 22 degrees in the laboratory. The spins and parities of the levels of interest and the nuclear configurations assumed for these states are shown in Table IV. Unlike the mass 13 states previously discussed, two-nucleon coefficients of fractional parentage based on intermediate coupling wave functions were not available for these reactions, so the nuclear structure factors were

computed on the basis of pure jj configurations. However, each configuration assumed is the dominant one expected from the single nucleon coefficients of fractional parentage relating mass 11 to mass 12.[22]

Figures 8 through 11 present experimental angular distributions and normalized DWBA fits for the levels shown in Table IV. The theory is normalized at a forward angle independently for each state in the spectrum. The optical model parameters used are given in Table II. The fits to the (p,t) angular distributions, with the possible exception of the 2.00 MeV ($1/2^-$) transition, are very good. Although the variation in quality of fit with change in the optical model parameters was studied, the "best fit" parameters for the ^{13}C reaction were just those used in the ^{15}N reaction, with a slight increase in the imaginary well radius for the outgoing triton, even though the incident beam energy in these two reactions differs by 6 MeV. Theoretical fits shown for the $(p,^3He)$ angular distributions in Figs. 8 through 11 are for a spin-independent interaction. We have not compared fits to the $(p,^3He)$ data for the cases of spin-independent vs. spin-dependent interactions, as was done for the $^{15}N(p,^3He)^{13}C$ transitions, because these mass 11 final state wave functions are too uncertain. The resultant $(p,^3He)$ fits are reasonable and should at least permit a comparison of (p,t) and $(p,^3He)$ cross sections, which, as noted earlier, appears to provide a sensitive test of the assumptions of the theory and/or the reaction mechanism.

As observed earlier for transitions to mass 13 final states, the DWBA calculation of the (p,t) and $(p,^3He)$ integrated cross sections to the several mass 11 mirror pairs, utilizing (p,t) nuclear structure factors for both, were

essentially equal so that theory and experiment can be directly compared for each mirror pair. Figure 12 presents such a comparison for the ground state transitions, where the cross sections in μb/sr are compared with theoretical predictions for the case of a spin-independent and the spin-dependent interaction. The theoretical curves are plotted in arbitrary units without relative normalization. As such, they represent how well the theory accounts for the relative magnitudes of these (p,t) and (p,^{3}He) transitions. Note that the agreement is much better with the inclusion of the strongly spin-dependent interaction. Similar comparisons have been made for the other strong states excited in the mass 11 final nuclei, and the ratios (R) of (p,t) to (p,^{3}He) integrated cross sections (the theory being integrated over the same range as the experiment) are shown in Table V. However, and unlike the ^{15}N results, relatively poor agreement is obtained for each mirror level, even in the limit of the strong spin dependence. Nevertheless, the results for these mass 11 final states are still consistent with what was found for the mass 13 final nuclei—that agreement between theory and experiment improves as one goes to a strongly spin-dependent interaction.

The most important results in Table V are the experimental ratios for the $1/2^-$ and $5/2^-$ integrated cross sections, both of which are well above the 4/1 limit expected for a pure S=0 transfer of the neutron-proton pair. The theoretical ratios for these transitions, even in the case of strong spin dependence, remain in very poor agreement with experiment. In order to emphasize this, the differential cross sections for these $1/2^-$ and $5/2^-$ (p,t) and (p,^{3}He) transitions are shown again in Fig. 13. At forward angles, where direct reaction contributions to the cross section are expected to be at a maximum, the (p,t) transition is favored over the (p,^{3}He) by factors as

large as six or seven.

There are now three examples where the ratios of (p,t) to (p,^{3}He) cross sections are beyond the limit predicted by theory. Table VI presents the total cross sections for these cases integrated just over the forward angles of the data and compares the results with those obtained over the total angular range considered earlier. Also shown are the theoretical predictions for the spin-independent interaction, integrated over the same angular range. For the mass 11 levels, the disagreement between theory and experiment is even more striking when considered over this limited angular range.

C. ^{31}P(p,t)^{29}P and ^{31}P(p,^{3}He)^{29}Si

Other data available on T=1/2 targets [those of ^{7}Li, ^{9}Be (Ref. 6); ^{27}Al, ^{31}P (Ref. 16); and ^{39}K (Ref. 17, 24)] are consistent with the previously mentioned general trend that, unless inhibited by nuclear structure considerations, the (p,t) transition is stronger than the corresponding mirror (p,^{3}He) transition. This is shown in Table VII where the experimental results for the cross section ratios of (p,t) and (p,^{3}He) reactions on these targets are given. Two values are shown: 1) the differential cross section ratio arising from the peak angle in the (p,t) reaction and the corresponding angle in the (p,^{3}He) reaction, and 2) the ratio of integrated cross sections over the angular range observed. Not shown are data concerning the "S-forbidden" transitions in the ^{9}Be(p,t)^{7}Be and ^{7}Li(p,t)^{5}Li reactions,[6] which are virtually absent in those spectra. The ratios which are close to unity in Table VII can presumably be understood on the basis of nuclear structure effects inhibiting

the (p,t) transition. Other than the striking cases of this inhibition discussed in Ref. 6, further examples may be found in Ref. 21.

Of the above data, the $^{31}P(p,t)^{29}P$ and $^{31}P(p,^{3}He)^{29}Si$ reactions appeared the most tractable for detailed consideration, since nuclear wave functions were available and two-nucleon spectroscopic factors were readily calculable. This experiment was performed by Hardy and Skyrme,[16] using the 40 MeV proton beam from the Rutherford Linac. The ground state angular distributions and DWBA fits are shown in Fig. 14. Although only a small angular range is covered by these data, it is still worthwhile to present the DWBA fits in order to show that the theory properly accounts for the experimental angular distributions. The calculated curves are arbitrarily normalized to the data and the optical model parameters used are given in Table II. Note that the (p,t) transition is again much stronger than the mirror $(p,^{3}He)$ transition, with their cross sections at the peak angle differing by about a factor of four. Nuclear structure factors have been calculated from wave functions[25] based on a model of three nucleons outside a ^{28}Si core. Figure 15 shows the ground state angular distribution compared with the theory for the spin-independent and spin-dependent nucleon-nucleon interaction discussed earlier. The theoretical curves represent the relative magnitude of these (p,t) and $(p,^{3}He)$ transitions and, as observed earlier, agreement with experiment is much improved for the case of a strongly spin-dependent nucleon-nucleon interaction.

IV. POSSIBLE EXPLANATIONS

Although the theory generally gives a good account of the shapes of

(p,t) angular distributions, it is unable, in almost every case, to account for the ratios of cross sections observed for (p,t) and (p,^{3}He) transitions to T=1/2 mirror states. We find that the introduction of a strongly spin-dependent force ($A^S = 0.3A^T$) considerably improves the agreement between theory and experiment for these ratios, but even so the overall average behavior of the data is not reproduced. Moreover, three examples now discussed lie outside the pure S=0 limit of the present theory. An explanation for these results is sought either in one, or both, of the following: 1) that the neglect of spin-dependent interactions in the optical potential is not justified or 2) that a two-step reaction mechanism may be competitive with the direct reaction mode.[26]

A. Coherence Arising from the Spin-orbit Interaction

The present theory assumes that the incident particle interacts only with the two nucleons to be transferred and has no other interactions except its interaction with the nucleus through the optical potential; the further assumption of the absence of spin-orbit coupling in the optical potential leads to an incoherent sum on all the angular momentum quantum numbers of the transferred pair. However, when a spin-orbit potential is included in the optical model, the orbital angular momentum (L) and the spin angular momentum (S) transferred in the reaction are no longer incoherent (although the sum on the total angular momentum (J) remains incoherent) and a coherent sum on these quantum numbers must be considered.[27]

The coherence introduced through the spin-orbit interaction will not affect the (p,t) reaction since, to first order, the spin transfer is zero.

The $(p,{}^3He)$ reaction, on the other hand, might be expected to undergo a considerable change since now a separation between the L and S transferred in the reaction cannot be achieved. In this case, representing the entrance and exit channel spins by S_a and S_b, respectively, the differential cross section can be written[27] as—

$$\frac{d\sigma}{d\Omega}(p,{}^3He) \propto \sum_{\substack{JM \\ m_a m_b}} \left| \sum_{M' m_a' m_b'} \sum_{LS} C_{ST} \left(\sum_N G_{NLSJT} B_{NL}^{M,M' m_a, m_a', m_b, m_b'} \right) \right|^2 \tag{8}$$

where the distorted wave amplitude now contains discrete sums over the channel spin projections (M', m_a', m_b'). (See Ref. 27 for a more complete discussion.)

The strong influence of the S=1 transfer in the $(p,{}^3He)$ reaction can be seen in those transitions in which it permits the reaction to proceed via multiple L transfers. For most of these cases the $(p,{}^3He)$ angular distribution is quite unlike the corresponding (p,t) transition where, in the cases discussed here, only a single L value is allowed. The coherence introduced through the spin-orbit interaction could have a marked effect on the $(p,{}^3He)$ cross section, possibly reducing it with respect to the mirror (p,t) transition, so that agreement between theory and experiment might be considerably

improved over what has been heretofore presented based on an incoherent sum.[28]

As previously discussed, our DWBA code cannot calculate the influence of such interference terms on the cross section, since it contains no spin-orbit potential. To get an indication of whether such interference terms could explain our results, a very preliminary analysis with the Oak Ridge code JULIE was conducted on the $^{15}N(p,t)$ and $(p,^3He)$ transitions populating the $5/2^-$ levels at 7.38 MeV in ^{13}N and 7.55 MeV in ^{13}C.[29] The results are only tentative, but we did find, using the optical potential given in Table II, a considerable improvement in the ratios of (p,t) to $(p,^3He)$ cross sections as compared to the previously discussed (incoherent sum) calculations, although a spin dependence was still required. Clearly, much more extensive and detailed theoretical analysis is necessary to establish any quantitative results on the significance of spin-orbit interference terms in two-nucleon transfer reactions.

B. Coherence Arising from Core Excitation

Core excitation processes of course present a plausible explanation for some j-forbidden transitions,[30-32] but it is also possible that the presence of such two-step processes could offer an alternative explanation for the ratios of (p,t) to $(p,^3He)$ cross sections that have been observed.

The best indication for the contribution of other mechanisms in these reactions would appear to be the $^{13}C(p,t)^{11}C$ $(7/2^-)$ transition. Assuming that ^{13}C can be represented by a pure $(1p)^9$ configuration, then transitions to a $7/2^-$ state by the direct pickup of a neutron pair are "J-forbidden" in the (p,t) reaction (see Ref. 21). Nevertheless, this level is relatively strongly excited in the spectrum (compare Fig. 7 and Table V) and its angular distribution

is shown in Fig. 16. Also shown in this figure is the angular distribution for the $^{15}N(p,t)^{13}N$ 6.38 MeV $(5/2^+)$ transition, which is also a forbidden transition for pickup in the (1p) shell. Both of these transitions have similar shapes, especially at forward angles, and it is provocative to consider them as arising largely through a two-step (core excitation) reaction mechanism. The ^{13}N 6.38 MeV $(5/2^+)$ transition is discussed in more detail in Ref. 21; here we discuss the $^{13}C(p,t)^{11}C$ $(7/2^-)$ transition. This level is also relatively strongly excited in the $^{12}C(d,t)^{11}C$ reaction where it is again j-forbidden and its population has been interpreted[19,32] as arising mostly through a core excitation pickup reaction. A compound nucleus mechanism is unlikely at these high bombarding energies and in general no evidence is seen for appreciable knock-out population of final states.[19,21,33]

Although the above evidence implies the presence of a two-step reaction mechanism, we have attempted to analyze this transition as if it arose through a direct (L=4) pickup of a (1p 1f) neutron pair. DWBA calculations were in fact able to reproduce the observed shape quite well and are presented in Ref. 21. Interestingly, this calculation also indicated that a 5% admixture of $(1f\ 7/2)^2$ in the ^{13}C ground state wave function could account for the strength of this $^{13}C(p,t)^{11}C$ $(7/2^-)$ transition. (This amount would be consistent with what is expected for $(1f\ 7/2)^2$ admixtures in 1p shell nuclei[34]). Mitigating against drawing this conclusion are 1) uncertainties in the DWBA treatment of such quantities as the bound state wave function for this type of transition and 2) the absence of relatively strong transitions to positive parity states arising from a presumably larger amount of $(2s1d)^2$ admixtures in the ^{13}C ground state. (The 6.90 MeV $(5/2^+)$ level of ^{11}C is populated strongest, but with a peak cross section of only 15 μb/sr). Considerably more detailed calculations would

be necessary to establish the origin of the population of this $7/2^-$ state.

Further suggestion of the presence of an interfering mechanism in these two-nucleon transfer reactions can be seen in the $^{13}C(p,^3He)^{11}B$ 4.44 MeV $(5/2^-)$ transition. Figure 17 presents this angular distribution along with the mirror (p,t) transition to the 4.32 MeV $(5/2^-)$ level in ^{11}C at two different beam energies, 43.7 MeV[33] and 49.7 MeV. Note that the small angle behavior of the $(p,^3He)$ angular distribution shown in Fig. 17 is reproduced at both energies. This transition is restricted to a pure L=2 transfer for both the (p,t) and $(p,^3He)$ reactions on the basis of a direct pick-up of two 1p nucleons. A typical L=2 shape is seen for the (p,t) transition,[21,33] which is well predicted by the DWBA calculations, while the $(p,^3He)$ cross section is poorly fit at forward angles (Fig. 10) and shows small angle behavior reminiscent of an L=0 transfer. The fact that this behavior appears in the $(p,^3He)$ angular distribution and not in the (p,t) merits further study, but could perhaps be accounted for by a core-excitation process which proceeds predominantly through the ^{13}C 3.68 MeV $(3/2^-)$ level.[35]

Of interest is the effect that contributions from a core excitation mechanism could have on the magnitude of the overall cross section for a given transition. Following the treatment given by Penny and Satchler,[31] a schematic expression for the total cross section can be written as

$$\sigma \propto |T_1 + T_2|^2 \propto |T_1|^2 + |T_2|^2 + 2\,\mathrm{Re}(T_1 \cdot T_2^*) \qquad (9)$$

where T_1 is the amplitude for the direct transition and T_2 is the amplitude for the core-excitation transition (including inelastic scattering). The last term in the above equation is an interference term between the direct and the

core excitation transitions. We have seen that the ^{11}C $7/2^-$ state is excited with an appreciable cross section, and insofar as this could be taken as evidence for a core excitation pick-up reaction, then interference effects could presumably be quite large. For a two-nucleon transfer reaction, in the absence of spin-orbit coupling, the orbital angular momentum L and total angular momentum J transferred in each reaction path will be coherent. Due to its additional allowed S=1 spin transfer, many more interference terms would be involved in a given $(p,^3He)$ transition than the corresponding mirror (p,t) transition. It is not clear whether such effects could account for the observed ratios of (p,t) and $(p,^3He)$ transitions to mirror final states.

V. SUMMARY

A spin dependence in the nucleon-nucleon interaction, somewhat stronger than what is generally used [13,15] has been introduced in the two-nucleon transfer DWBA treatment in an attempt to reproduce the observed ratios of mirror (p,t) to $(p,^3He)$ cross sections. Generally speaking, this led to a modification of the computed ratio in the correct direction but did not in itself provide a satisfactory account of the data. Several transitions were observed in which this ratio was greater than the 4/1 limit expected for pure S=0 transfer of the nucleon pairs and interference terms arising through either spin-orbit coupling in the optical potential or through core excitation were suggested as accounting for this result. The former explanation is somewhat preferred, especially when one notes that the examples which are outside this limit arise from highly populated final states. [They involve the strongest transition in the $^{15}N(p,t)^{13}N$ data and the second and third strongest in the $^{13}C(p,t)^{11}C$

data]. Either, or both, could also, of course, act in addition to the spin-dependent interaction in explaining the majority of the data which involve experimental ratios less than 4/1.

In summary, then, if core excitation is sufficiently probable and if the parentage of the final state has a large component based on the excited core, then this must be taken into account in a calculation of the reaction cross section. This applies both to the (p,t) and the (p,^{3}He) reactions. The DWBA can be extended to include such effects,[31] though most available codes do not include them. On the other hand, the coherence introduced through spin-orbit coupling in the optical potential does not alter the (p,t) reaction and applies only to the (p,^{3}He) reaction <u>when</u> the (LS) angular momentum quantum numbers of the transferred pair can interfere (e.g., in most T=1/2 to T=1/2 transitions). In fact, until this latter problem is understood, the spectroscopic utility of (p,^{3}He) or (^{3}He,p) reactions on T≠0 targets is greatly hampered. It appears that the presence of interference terms in these two-nucleon transfer reactions has been demonstrated and therefore must be calculated in order to properly explain the experimental results.

FOOTNOTES AND REFERENCES

1) J. Cerny and R. H. Pehl, Phys. Rev. Letters 12, 619 (1964).

2) C. Detraz, J. Cerny, and R. H. Pehl, Phys. Rev. Letters 14, 708 (1965); J. Cerny, R. H. Pehl, G. Butler, D. G. Fleming, C. Maples, and C. Detraz, Phys. Letters 20, 35 (1966).

3) J. Cerny, R. H. Pehl, and G. T. Garvey, Phys. Letters 12, 234 (1964); G. T. Garvey, J. Cerny, and R. H. Pehl, Phys. Rev. Letters 12, 726 (1964).

4) N. K. Glendenning, Ann. Rev. Nucl. Science 13, 191 (1963); N. K. Glendenning, Phys. Rev. 137B, 102 (1965).

5) J. R. Rook and D. Mitra, Nucl. Phys. 51, 96 (1964); C. L. Lin and S. Yoshida, Prog. Theor. Phys. (Tokyo) 32, 885 (1964); E. M. Henley and D. V. L. Yu, Phys. Rev. 133B, 1445 (1964); B. Bayman, Argonne National Laboratory Report, ANL-6878, 335 (1964) (unpublished); A. Y. Abul-Magd and M. El Nadi, Nucl. Phys. 77, 182 (1966); V. S. Mathur and J. R. Rook, Nucl. Phys. A91, 305 (1967).

6) J. Cerny, C. Detraz, and R. H. Pehl, Phys. Rev. 152, 950 (1966).

7) N. F. Mangelson and B. G. Harvey, Lawrence Radiation Laboratory Annual Report UCRL-17299, 97 (1966) (unpublished), and private communication.

8) N. K. Glendenning, Phys. Rev. 156, 1344 (1967).

9) J. J. Wesolowski, L. F. Hansen, J. G. Vidal, and M. L. Stelts, Phys. Rev. 148, 1063 (1966); J. Vervier, Phys. Letters 22, 82 (1966); R. A. Broglia and C. Riedel, Nucl. Phys. A92, 145 (1967).

10) J. M. Blatt, G. H. Derrick, and J. N. Lyness, Phys. Rev. Letters 8, 323 (1962); R. Pascual, Phys. Letters 19, 221 (1965); B. F. Gibson, Phys. Rev. 139, 1153 (1965).

11) J. L. Gammel and R. M. Thaler, Phys. Rev. 107, 291, 1337 (1957); P. S. Signel and R. E. Marshak, Phys. Rev. 109, 1229 (1958); K. E. Lassila, M. J. Hull, H. M. Ruppel, F. A. McDonald, and G. Breit, Phys. Rev. 126, 881

(1962); T. Hamada and I. D. Johnston, Nucl. Phys. 34, 383 (1962).

12) C. L. Storrs and D. H. Frisch, Phys. Rev. 95, 1252 (1954); L. Hulthen and M. Sugawara, Encyc. of Physics (Handbuch der Physik) 39, 1 (1957); M. A. Preston, "Physics of the Nucleus," Addison - Wesley Publishing Co., 25 (1962).

13) W. J. S. Y. Young, Nucl. Phys. 55, 84 (1964).

14) T. T. S. Kuo and G. E. Brown, Nucl. Phys. 85, 40 (1966); N. Freed and P. Goldhammer, Phys. Letters 23, 564 (1966); G. E. Brown and T. T. S. Kuo, Nucl. Phys. A92, 481 (1967).

15) S. G. Nillson, J. Sawicki, and N. K. Glendenning, Nucl. Phys. 33, 239 (1962); A. Kallio and K. Kolltveit, Nucl. Phys. 53, 87 (1964).

16. J. C. Hardy and D. J. Skyrme, University of Oxford Report, Physics Laboratory, No. 189 (1966).

17. G. Butler, J. Cerny, S. W. Cosper, and R. L. McGrath, submitted to the Physical Review.

18) We would also expect this ratio to be unity for mirror single nucleon transitions, and this has been recently verified in the $^{12}C(d,t)^{11}C$ and $^{12}C(d,^3He)^{11}B$ reactions. (See Ref. 19).

19) M. Chabre, D. L. Hendrie, H. G. Pugh, and C. Detraz, Lawrence Radiation Laboratory Annual Report UCRL-16580, 68 (1965) (unpublished).

20) Actually, the ratio would be slightly greater than this (about 4.1) since the spatial overlap between the A=3 ground state and the transferred pair is slightly greater for tritons than for ^3He (see Ref. 4 or Ref. 21).

21) D. G. Fleming, J. Cerny, C. C. Maples, and N. K. Glendenning, to be submitted to the Physical Review.

22) S. Cohen and D. Kurath, Nucl. Phys. 73, 1 (1965); D. Kurath, private communication.

23) In the majority of cases, the $(p,{}^3He)$ transitions were 5 to 10% larger than the corresponding mirror (p,t) transitions. In no case was the (p,t) transition more than 5% greater than the mirror $(p,{}^3He)$ transition.

24) J. Cerny, et al., unpublished data.

25) P. W. M. Glaudemans, G. Wichers, and P. J. Brussard, Nucl. Phys. 56, 548 (1964).

26) Other processes than the ones we have considered may be important in these reactions. For example, the small $^4D_{1/2}$ component[10] of the ground state A=3 wave function could introduce additional angular momenta as well as interference terms into both the (p,t) and $(p,{}^3He)$ transitions.

27) G. R. Satchler, Nucl. Phys. 55, 1 (1964).

28) These interference terms should also, in general, alter the shape of the $(p,{}^3He)$ angular distribution, but it appears that such effects might not be very large in view of the relatively good fits already obtained in the $^{15}N(p,{}^3He)^{13}C$ reaction.

29) JULIE also differs from our code in that it does not contain a coherent sum on the principal quantum number N. However, this is of no consequence for these $5/2^-$ (L=2) transitions, since N=1 is the only term allowed by selection rules.

30) R. Bock, H. H. Duhm, R. Rudel, and R. Stock, Phys. Letters 13, 151 (1964); T. A. Belote, W. E. Dorenbusch, O. Hansen, and J. Rapaport, Nucl. Phys. 73, 321 (1965); B. Kozlowsky and A. De-Shalit, Nucl. Phys. 77, 215 (1966); S. K. Penny, Thesis, University of Tennessee (unpublished) (1966); F. S. Levin, Phys. Rev. 147, 715 (1966).

31) S. K. Penny and G. R. Satchler, Nucl. Phys. 53, 145 (1964).

32) D. Kurath, Proceedings of the Gatlinburg Conference on Nuclear Physics (to be published) (1967).

33) D. G. Fleming, Ph.D. thesis, University of California (Berkeley), (1967).

34) D. Kurath, Phys. Rev. 140, 1190 (1965); D. H. Wilkinson, J. T. Sample, and D. E. Alburger, Phys. Rev. 146, 662 (1966).

35) This $3/2^-$ level is strongly excited in the $^{13}C(\alpha,\alpha')^{13}C$ reaction at 40 MeV (B. G. Harvey, J. R. Meriwether, J. Mahoney, A. Bussiere de Nercy, and D. J. Horen, Phys. Rev. 146, 712 (1966)). Transitions through this level could also account for the population of the 6.49 MeV $(7/2^-)$ level in the $^{13}C(p,t)^{11}C$ reaction.

Table I. Mass 13 Levels and Major Intermediate Coupling Configurations

J^π	^{13}N Exc. (MeV)	^{13}C Exc. (MeV)	Major Configurations[a]
$1/2^-$	0	0	$.501(p_{3/2})^6_0(p_{1/2})^3 + .837(p_{3/2})^8_0 p_{1/2}$
$3/2^-$	3.51	3.68	$.450(p_{3/2})^5(p_{1/2})^4_0 - .733(p_{3/2})^7(p_{1/2})^2_0$
$5/2^-$	7.38	7.55	$.313(p_{3/2})^6_2(p_{1/2})^3 - .929(p_{3/2})^7(p_{1/2})^2_1$

[a] See Ref. 22. We are indebted to Dr. Kurath for providing us with these wave functions.

Table II. Optical Model Potentials

$$-U(r) = Vf(r) + i4aW_d f'(r) + iWf(r) - V_c(r)$$

Channel	V	W_D	a	a_w	r	r_w	r_c
$^{15}N + p$	34	22	.65	.50	1.25	1.25	1.30
$^{13}N + t$ $^{13}C + {}^3He$	153	16	.65	.54	1.25	1.25	1.30
$^{13}C + p$	34	22	.65	.50	1.25	1.25	1.30
$^{11}C + t$ $^{11}B + {}^3He$	153	16	.65	.54	1.25	1.45	1.30
$^{31}P + p$	41.7	11.1[a]	.70	.70	1.20	1.20	1.30
$^{29}P + t$ $^{29}Si + {}^3He$	153	16	.65	.54	1.25	1.50	1.30

[a] Volume absorption was used

Table III. Mass 13 Experimental and Theoretical Integrated Cross Sections, (10-90°, cm)

J^π	$\sigma_T^{(p,t)}$ (μb)	$\sigma_T^{(p,{}^3He)}$ (μb)	$R_{exp}=\frac{\sigma_T(p,t)}{\sigma_T(p,{}^3He)}$	$R_{theo.}$ $A^S=A^T$	$R_{theo.}$ $A^S=0.3A^T$
$1/2^-$	941	308	3.06	.635	1.46
$3/2^-$	652	573	1.14	.686	1.50
$5/2^-$	1271	270	4.72	1.71	2.72

Table IV. Mass 11 Levels and Assumed jj Configurations

J^π	^{11}C Exc. (MeV)	^{11}B Exc. (MeV)	Configuration
$3/2^-$	0	0	$(p_{3/2})^7$
$1/2^-$	2.00	2.12	$(p_{3/2})^6_0\ p_{1/2}$
$5/2^-$	4.32	4.44	$(p_{3/2})^6_2\ p_{1/2}$
$3/2^-$	4.80	5.02	$(p_{3/2})^6_2\ p_{1/2}$

Table V. Mass 11 Experimental and Theoretical Integrated Cross Sections, (10-80°, cm)

J^π	$\sigma_T(p,t)$ (μb)	$\sigma_T(p,{}^3He)$ (μb)	$\frac{\sigma_T(p,t)}{R_{exp}=\sigma_T(p,{}^3He)}$	$R_{theo.}$ $A^S=A^T$	$R_{theo.}$ $A^S=0.3A^T$
$3/2^-$	1320	359	3.68	1.34	2.44
$1/2^-$	310	63	4.92	1.51	2.74
$5/2^-$	425	90	4.72	.402	1.01
$3/2^-$	167	58	2.88	.875	1.84
$7/2^-$	167	610	0.27	----	----

Table VI. Integrated (p,t)/(p,^{3}He) Cross Section Ratios for Those Levels Exceeding the Pure ^{13}S Transfer Limit of the Theory

	J^π	Excitation (MeV)	R(10-90°) experiment	R(10-45°) experiment	$A^S = A^T$ R(10-45°) theory
^{13}N	$5/2^-$	7.38	4.72	4.44	1.66
^{13}C		7.55			
^{11}C	$1/2^-$	2.00	4.92	5.88	1.55
^{11}B		2.12			
^{11}C	$5/2^-$	4.32	4.72	5.64	0.38
^{11}B		4.44			

Table VII. $(p,t)/(p,{}^3He)$ Cross Section Ratios for Other Data Available on T=1/2 Targets

	Reaction	J^π	Excitation[a] (MeV)	Peak[b] Angle Ratio	Integrated (σ_T) Ratio	Ref.
^7Li	$\rightarrow {}^5Li, {}^5He$	$3/2^-$	g.s.	3.0	2.3	6
^9Be	$\rightarrow {}^7Be, {}^7Li$	$3/2^-$	g.s.	3.3	2.5	6
	$\rightarrow {}^7Be^*, {}^7Li^*$	$1/2^-$	0.478	2.9	1.5	6
	$\rightarrow {}^7Be^*, {}^7Li^*$	$7/2^-$	4.63	1.8	1.3	6
^{27}Al	$\rightarrow {}^{25}Al, {}^{25}Mg$	$5/2^+$	g.s.	3.7	3.3	16
	$\rightarrow {}^{25}Al^*, {}^{25}Mg^*$	$7/2^+$	1.61	2.0	1.9	16
^{31}P	$\rightarrow {}^{29}P, {}^{29}Si$	$1/2^+$	g.s.	4.1	3.0	16
	$\rightarrow {}^{29}P^*, {}^{29}Si^*$	$5/2^+$	2.04	1.0	0.80	16
^{39}K	$\rightarrow {}^{37}K, {}^{37}A$	$3/2^+$	g.s.	4.5	3.8	17,24

[a] For low Z member of the mirror pair

[b] First maximum beyond zero degrees in the (p,t) transition.

FIGURE CAPTIONS

Fig. 1 Energy spectra for the $^{15}N(p,t)^{13}N$ and $^{15}N(p,^3He)^{13}C$ reactions at 22 deg. The spectra have been adjusted to match the ground state channels, showing a slight non-linearity in the higher energy tritons.

Fig. 2 Angular distributions for transitions to the ground states of ^{13}N and ^{13}C populated in the $^{15}N(p,t)$ and $(p,^3He)$ reactions, respectively. The curves are DWBA fits to the data for a spin independent nucleon-nucleon interaction, $A^S=A^T$. The theoretical curves have been separately and arbitrarily normalized to the data at forward angles. The optical model parameters used were the same for tritons and helium-3 and are given in Table II.

Fig. 3 Angular distributions of (p,t) and $(p,^3He)$ transitions to the 3.51 MeV and 3.68 MeV $(3/2^-)$ levels in ^{13}N and ^{13}C, respectively. As in Fig. 2, the curves represent DWBA fits to the data.

Fig. 4 Angular distributions of (p,t) and $(p,^3He)$ transitions to the 7.38 and 7.55 MeV $(5/2^-)$ levels in ^{13}N and ^{13}C, respectively. As in Fig. 2, the curves represent DWBA fits to the data.

Fig. 5 DWBA fits to the $^{15}N(p,^3He)^{13}C$ ground state $(1/2^-)$ and 3.68 MeV $(3/2^-)$ transitions, utilizing the spin-dependent nucleon-nucleon interaction, $A^S=0.3A^T$. The theoretical curves have been arbitrarily and separately normalized to the data at a forward angle.

Fig. 6 a) $^{15}N(p,t)^{13}N$ and $^{15}N(p,^3He)^{13}C$ ground state $(1/2^-)$ angular distributions. The curves are drawn through the experimental points and have no theoretical significance.

b) Theoretical cross sections for a spin independent $(A^S=A^T)$ nucleon-nucleon interaction. The dashed line represents the $^{15}N(p,t)^{13}N$

ground state transition and the solid line the $^{15}N(p,^3He)^{13}C$ ground state transition. The cross sections are given in the same arbitrary units and have not been normalized to each other.

c) As in b), but with the spin-dependent ($A^S=0.3A^T$) nucleon-nucleon interaction.

Fig. 7 Energy spectra for the $^{13}C(p,t)^{11}C$ and $^{13}C(p,^3He)^{11}B$ reactions at 22 deg. (lab.). The spectra have been adjusted to match channels for the $7/2^-$ levels, showing a slight non-linearity in the triton energy spectrum at the higher energies.

Fig. 8 Angular distributions for transitions to the ground states of ^{11}C and ^{11}B populated in the $^{13}C(p,t)$ and $(p,^3He)$ reactions, respectively. The curves represent DWBA fits to the data for a spin-independent nucleon-nucleon interaction. The theoretical curves have been separately and arbitrarily normalized to the data at forward angles. Optical model parameters used were the same for tritons and helium-3 and are given in Table II.

Fig. 9 Angular distributions for transitions to the 2.00 MeV and 2.12 MeV ($1/2^-$) levels in ^{11}C and ^{11}B, respectively. As in Fig. 8, the curves represent DWBA fits to the data.

Fig. 10 Angular distributions for transitions to the 4.32 MeV and 4.44 MeV ($5/2^-$) levels in ^{11}C and ^{11}B, respectively. As in Fig. 8, the curves represent DWBA fits to the data.

Fig. 11 Angular distributions for transitions to the 4.80 MeV and 5.02 MeV ($3/2^-$) levels in ^{11}C and ^{11}B, respectively. As in Fig. 8, the curves represent DWBA fits to the data.

Fig. 12 a) The $^{13}C(p,t)^{11}C$ and $^{13}C(p,^3He)^{11}B$ ground state $(3/2^-)$ angular distributions. The curves are drawn through the experimental points and have no theoretical significance.

b) Theoretical cross sections for a spin-independent $(A^S=A^T)$ nucleon-nucleon interaction. The dashed line represents the $^{13}C(p,t)^{11}C$ ground state transition and the solid line the $^{13}C(p,^3He)$ ^{11}B ground state transition. The cross sections are given in the same arbitrary units and have not been normalized to each other.

c) As in b), but with the spin-dependent $(A^S=0.3A^T)$ nucleon-nucleon interaction.

Fig. 13 a) the $^{13}C(p,t)^{11}C$ 2.00 MeV and the $^{13}C(p,^3He)^{11}B$ 2.12 MeV $(1/2^-)$ angular distributions. The curves are drawn through the experimental points and have no theoretical significance.

b) The angular distributions of the $^{13}C(p,t)^{11}C$ 4.32 MeV and the $^{13}C(p,^3He)^{11}B$ 4.44 MeV $(5/2^-)$ transitions. The curves have no theoretical significance.

Fig. 14 Angular distributions for the $^{31}P(p,t)^{29}P$ and $^{31}P(p,^3He)^{29}Si$ ground state $(1/2^+)$ transitions.[16] The curves represent DWBA fits to the data utilizing the spin independent $(A^S=A^T)$ nucleon-nucleon interaction. The theoretical curves have been separately and arbitrarily normalized at the peak angle. The optical model parameters used were the same for tritons and helium-3 and are given in Table II.

Fig. 15 a) Angular distributions for the $^{31}P(p,t)^{29}P$ and $^{31}P(p,^3He)$ ^{29}Si ground state $(1/2^+)$ transitions. The curves have no theoretical significance.

b) Theoretical cross sections for a spin-independent ($A^S=A^T$) nucleon-nucleon interaction. The dashed line represents the $^{31}P(p,t)^{29}P$ ground state transition and the solid line the $^{31}P(p,^3He)^{29}Si$ ground state transition. The cross sections are given in arbitrary units and have not been normalized to each other. c) As in b), but with the spin-dependent ($A^S=0.3A^T$) nucleon-nucleon interaction.

Fig. 16 Angular distributions for the $^{13}C(p,t)^{11}C$ 6.49 MeV ($7/2^-$) and the $^{15}N(p,t)^{13}N$ 6.38 MeV ($5/2^+$) transitions. The curves have no theoretical significance.

Fig. 17 Angular distributions for the $^{13}C(p,t)^{11}C$ 4.32 MeV and the $^{13}C(p,^3He)^{11}B$ 4.44 MeV ($5/2^-$) transitions, at incident proton energies of a) 43.7 and b) 49.6 MeV. The curves have no theoretical significance.

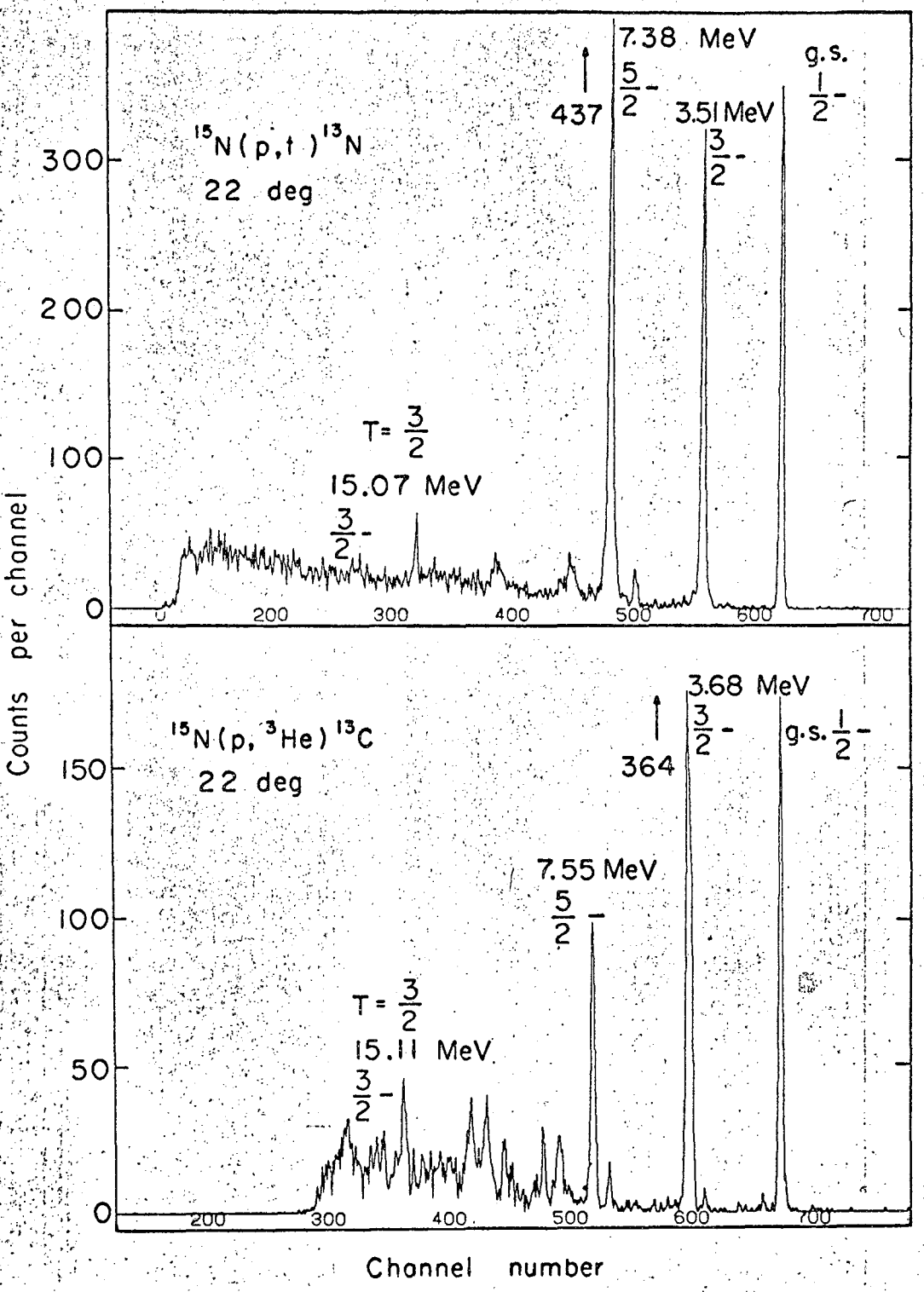
$^{15}N(p,t)^{13}N$
22 deg
437
7.38 MeV
5/2-
3.51 MeV
3/2-
g.s.
1/2-
T= 3/2
15.07 MeV
3/2-
$^{15}N(p,^3He)^{13}C$
22 deg
364
3.68 MeV
3/2-
g.s. 1/2-
7.55 MeV
5/2-
T = 3/2
15.11 MeV
3/2-
Counts per channel
Channel number
MUB-4742-A

Fig. 1

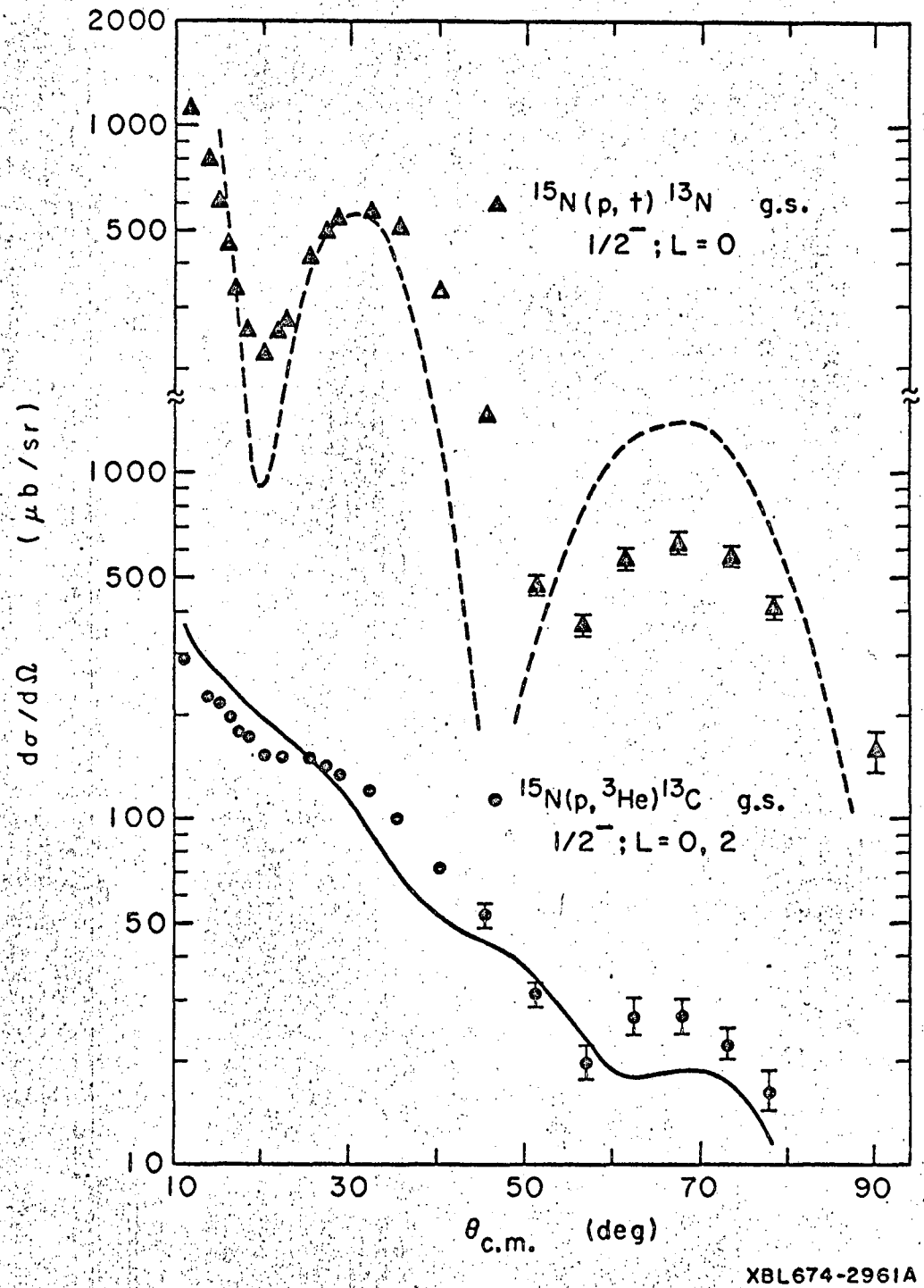
2000
1000
500
1000
500
100
50
10
10
30
50
70
90
dσ/dΩ (μb/sr)
θc.m. (deg)
15N(p, t) 13N g.s.
1/2⁻; L = 0
15N(p, 3He)13C g.s.
1/2⁻; L = 0, 2
XBL674-2961A

Fig. 2

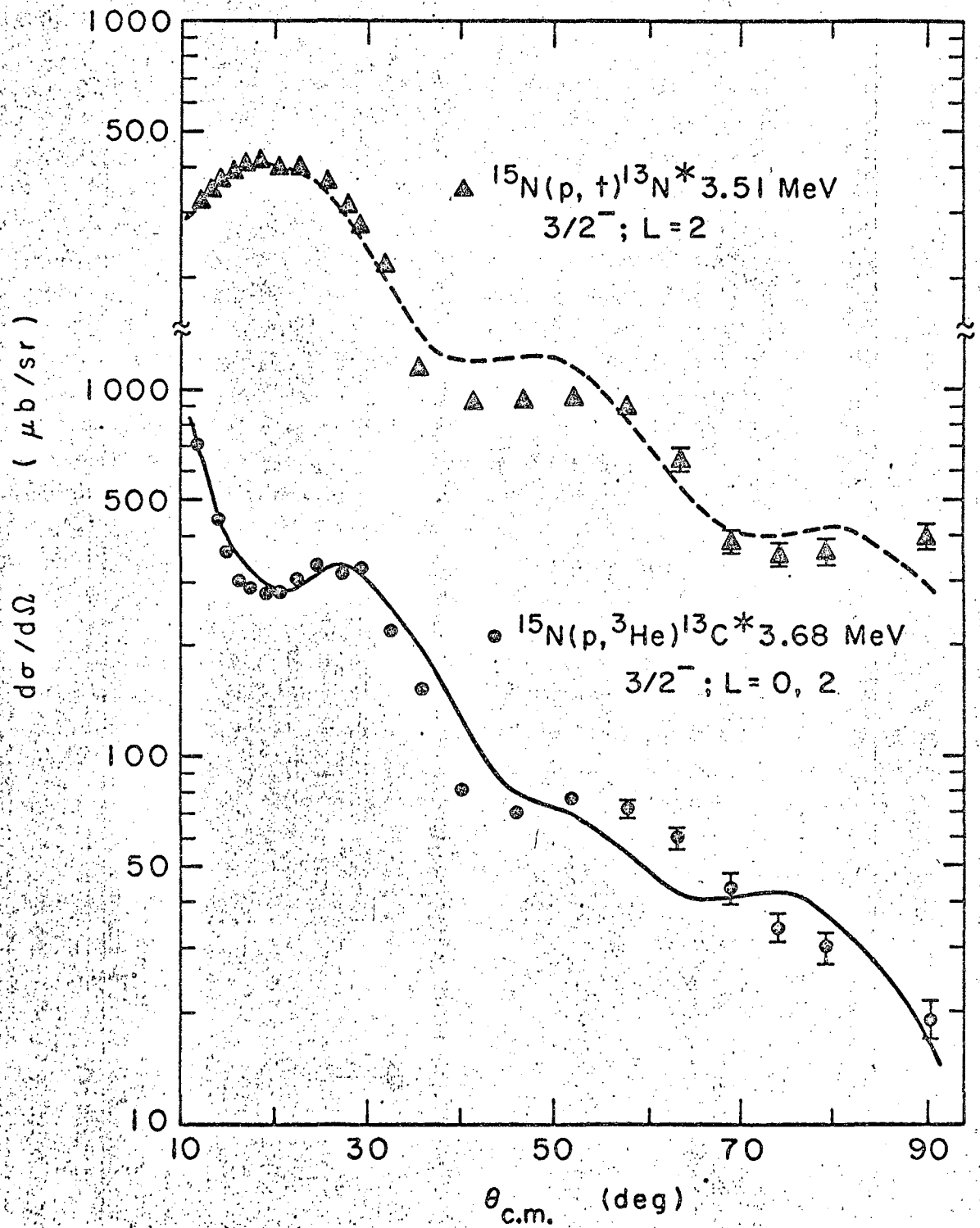

Fig. 3

XBL674-2960-A

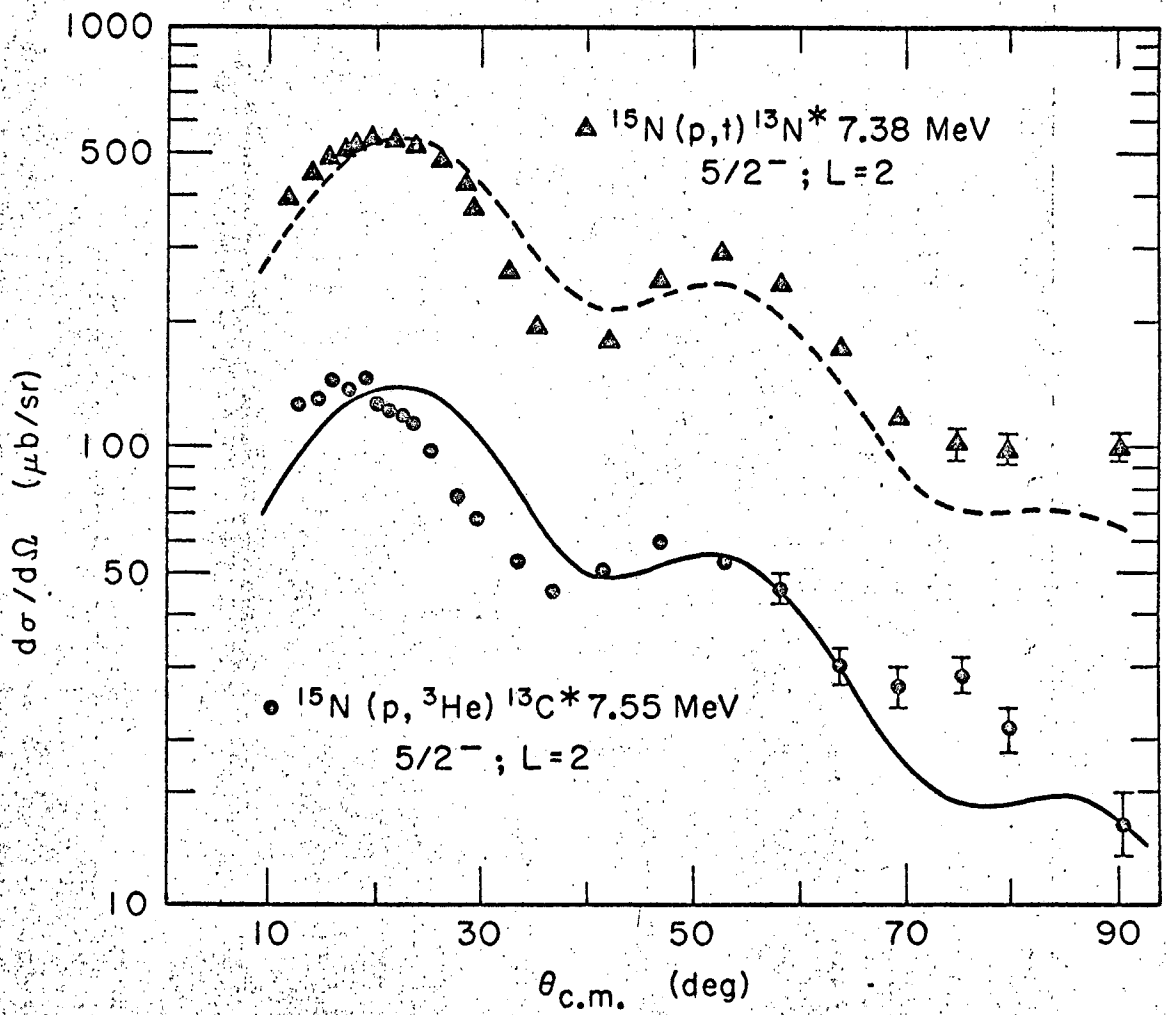
1000
500
100
50
10
10
30
50
70
90
dσ/dΩ (μb/sr)
θc.m. (deg)
△ 15N (p,t) 13N* 7.38 MeV
5/2⁻ ; L=2
● 15N (p, 3He) 13C* 7.55 MeV
5/2⁻ ; L=2
XBL676-3274-A

Fig. 4

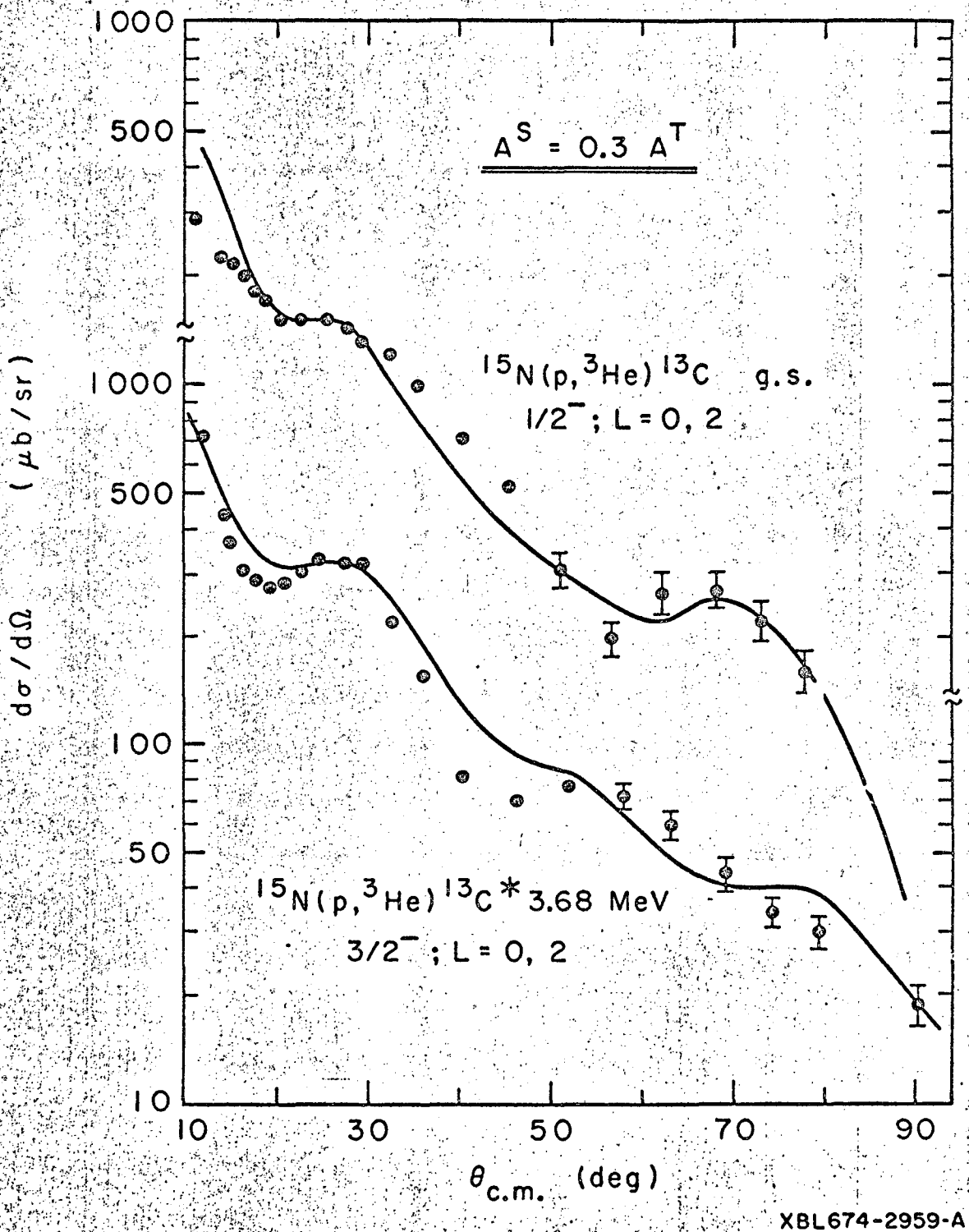
$A^S = 0.3\ A^T$
$^{15}N(p,^3He)\,^{13}C$ g.s.
1/2⁻; L = 0, 2
$^{15}N(p,^3He)\,^{13}C^*$ 3.68 MeV
3/2⁻; L = 0, 2
dσ/dΩ (μb/sr)
$\theta_{c.m.}$ (deg)
1000
500
100
50
10
30
70
90
XBL674-2959-A

Fig. 5

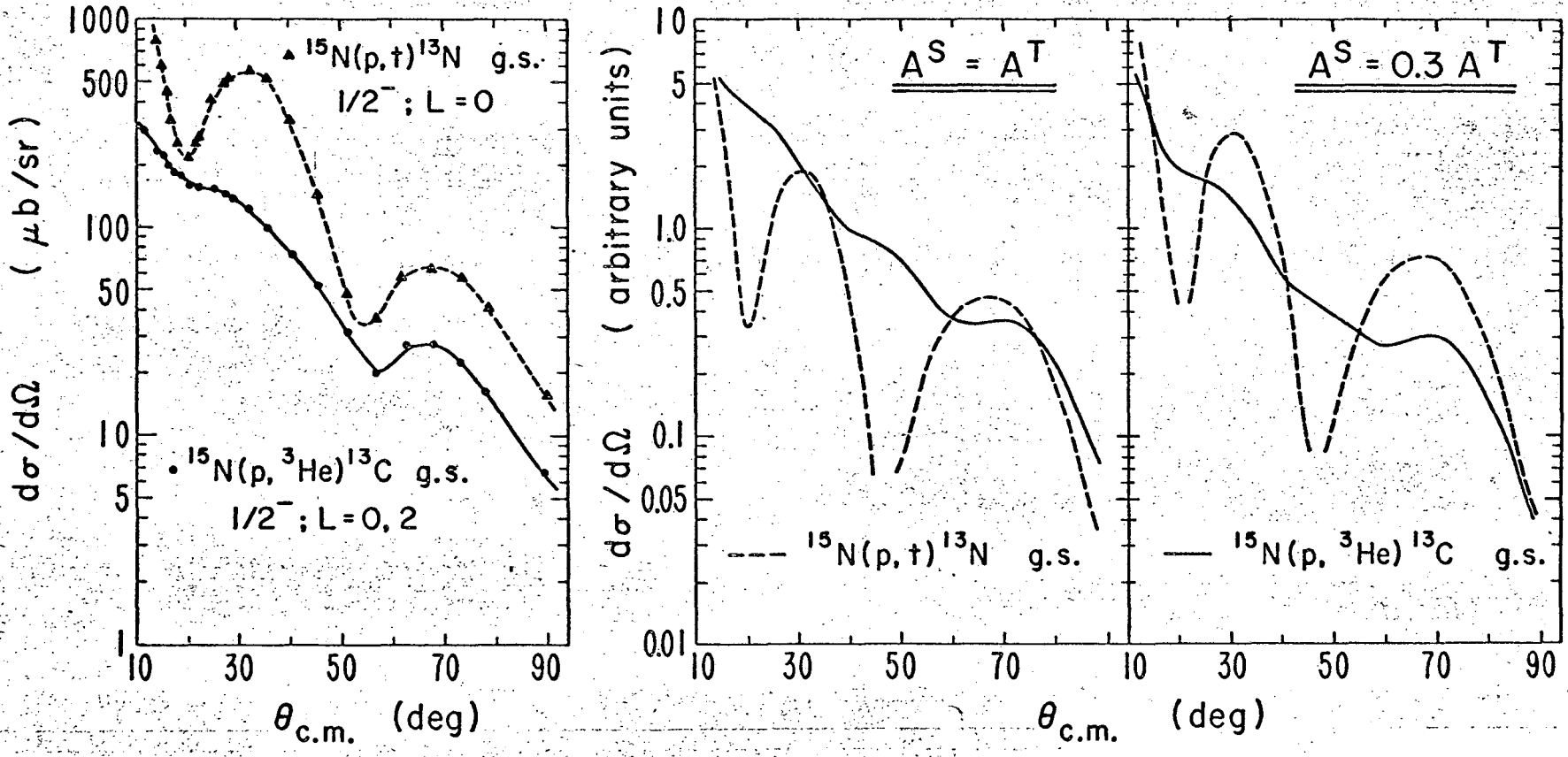
1000
500
100
50
10
5
1
dσ/dΩ (μb/sr)
▲ 15N(p,t)13N g.s.
1/2⁻; L=0
• 15N(p, 3He)13C g.s.
1/2⁻; L=0, 2
10
30
50
70
90
θc.m. (deg)
10
5
1.0
0.5
0.1
0.05
0.01
dσ/dΩ (arbitrary units)
AS = AT
AS = 0.3 AT
--- 15N(p,t)13N g.s.
— 15N(p, 3He)13C g.s.
θc.m. (deg)
XBL674-2972-A

Fig. 6

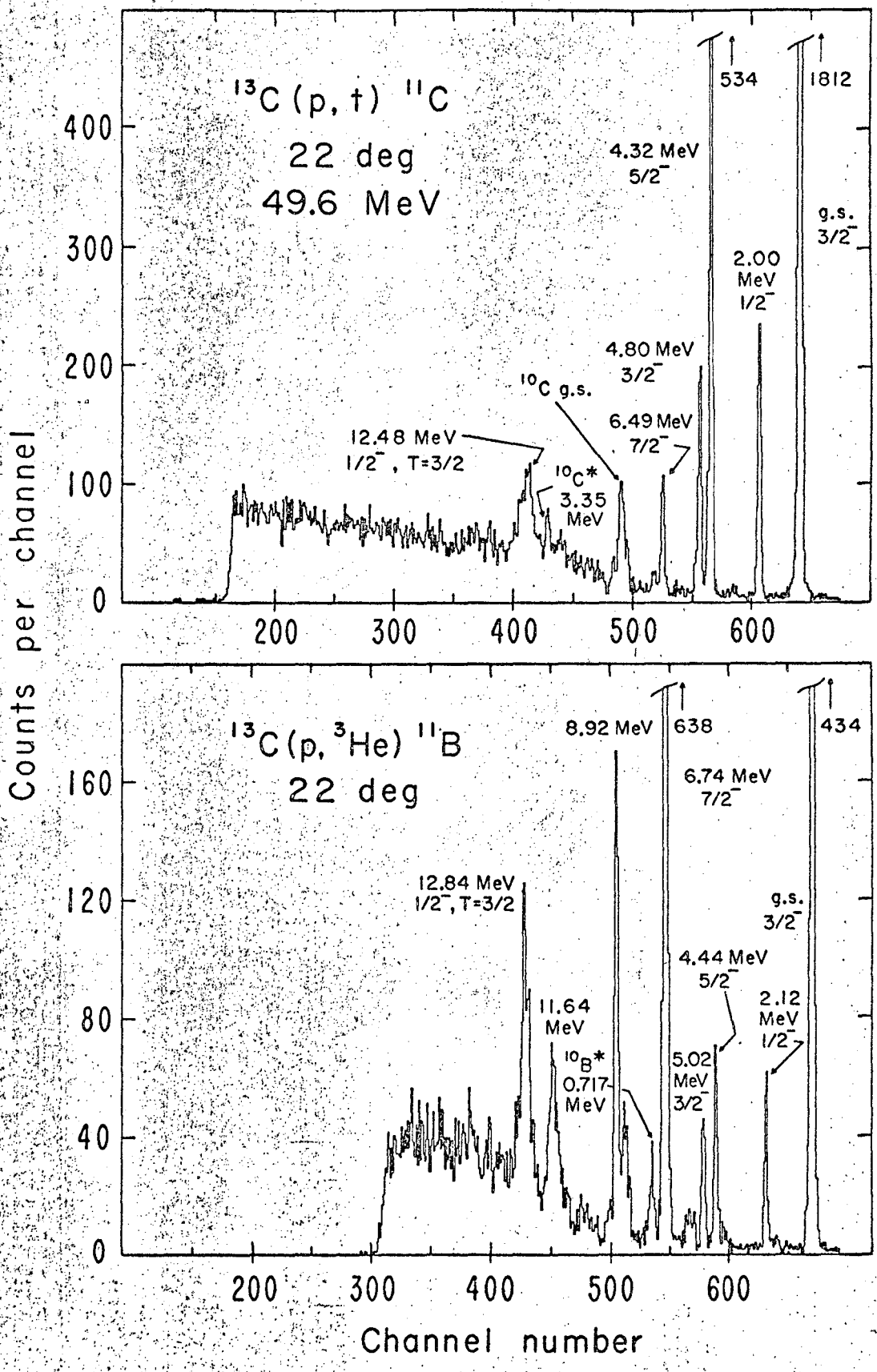

XBL677-3551

Fig. 7

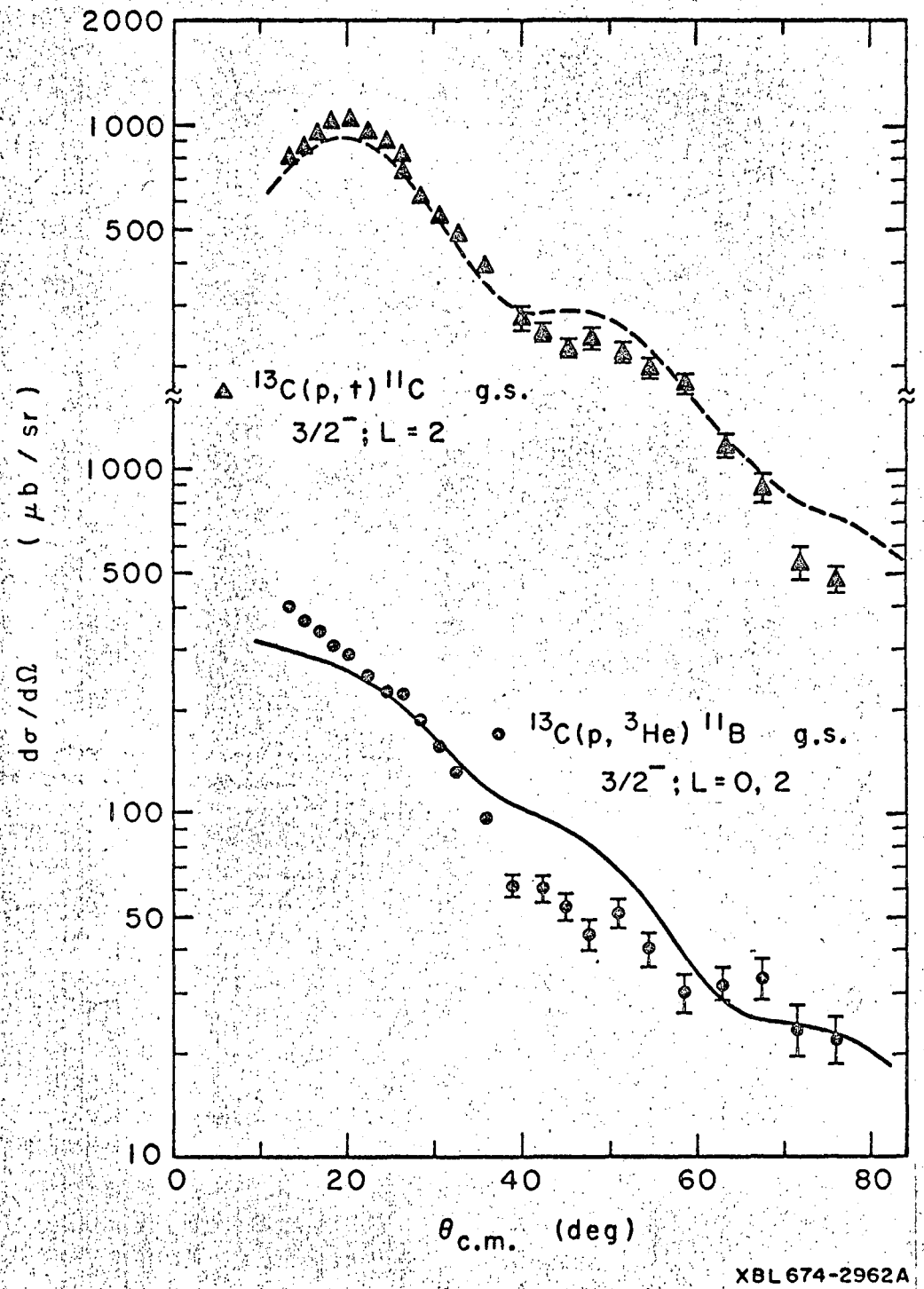
2000
1000
500
1000
500
100
50
10
0
20
40
60
80
dσ/dΩ (μb/sr)
θc.m. (deg)
△ 13C(p, t)11C g.s.
3/2⁻; L = 2
○ 13C(p, 3He)11B g.s.
3/2⁻; L = 0, 2
XBL674-2962A

Fig. 8

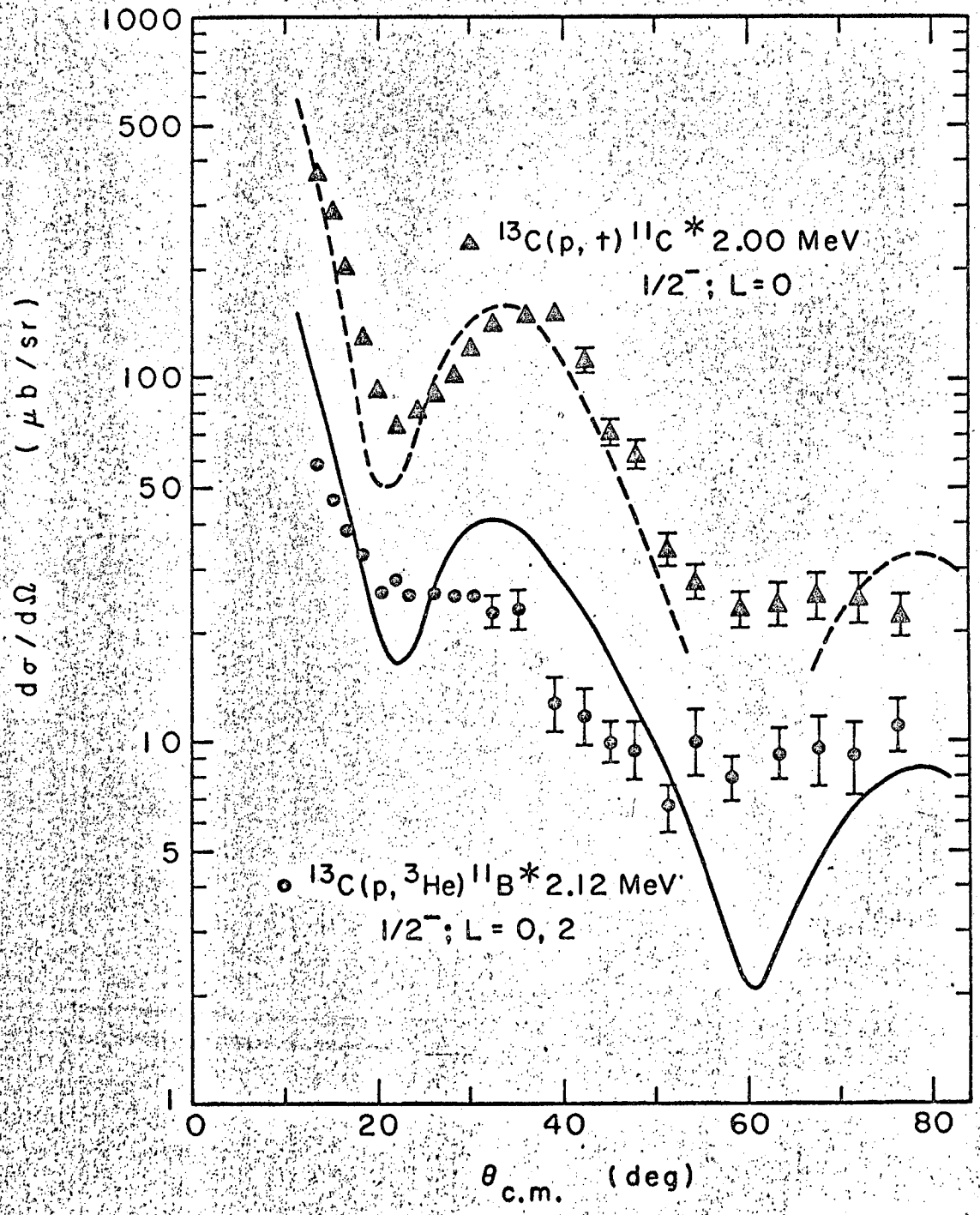
1000
500
100
50
10
5
1
0
20
40
60
80
dσ/dΩ (μb/sr)
θc.m. (deg)
13C(p, t)11C* 2.00 MeV
1/2⁻; L=0
13C(p, 3He)11B* 2.12 MeV
1/2⁻; L = 0, 2
XBL674-2964

Fig. 9

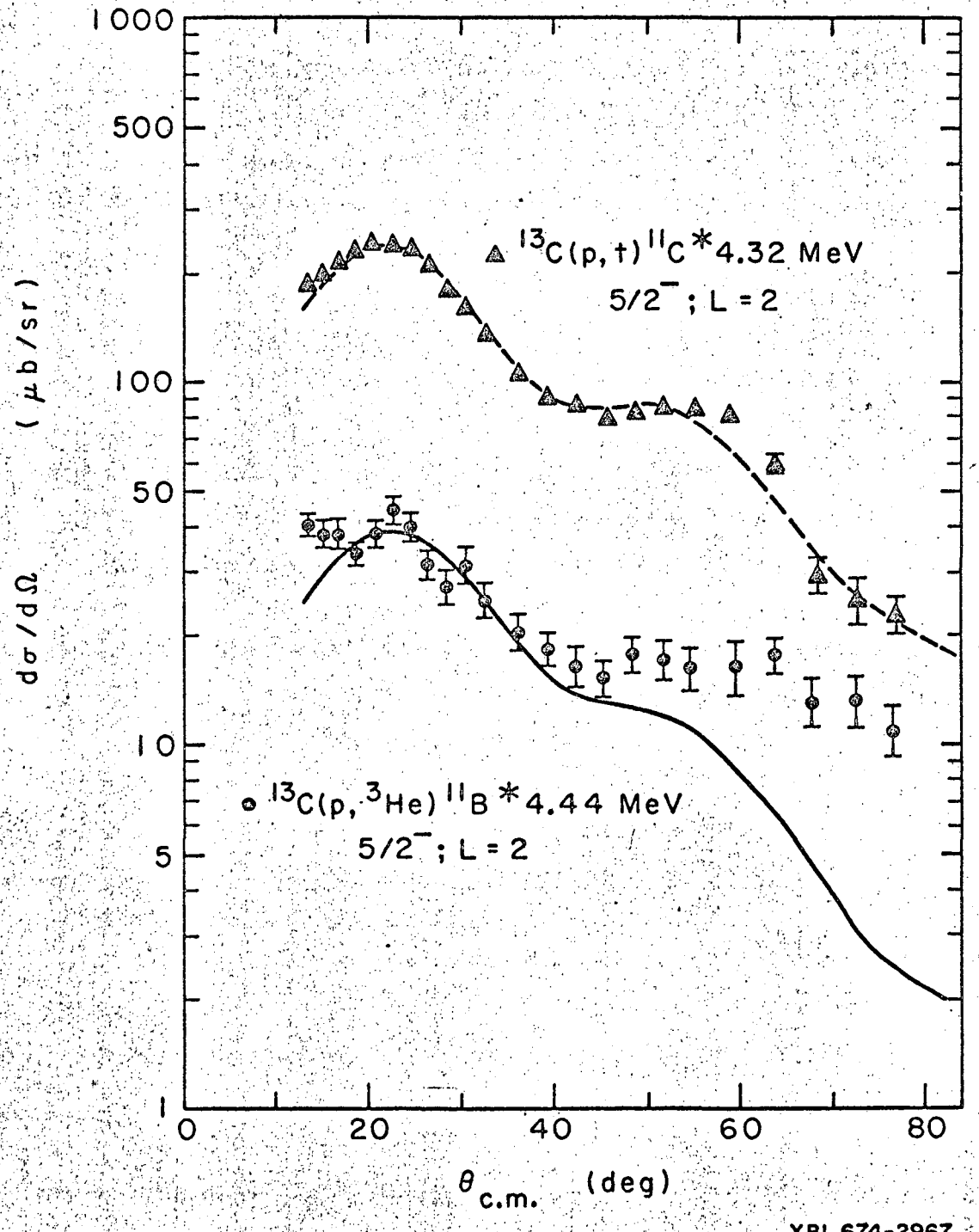
1000
500
100
50
10
5
1
0
20
40
60
80
dσ/dΩ (μb/sr)
θ c.m. (deg)
$^{13}C(p,t)^{11}C^*$4.32 MeV
5/2⁻; L = 2
$^{13}C(p,^3He)^{11}B^*$4.44 MeV
5/2⁻; L = 2
XBL 674-2967

Fig. 10

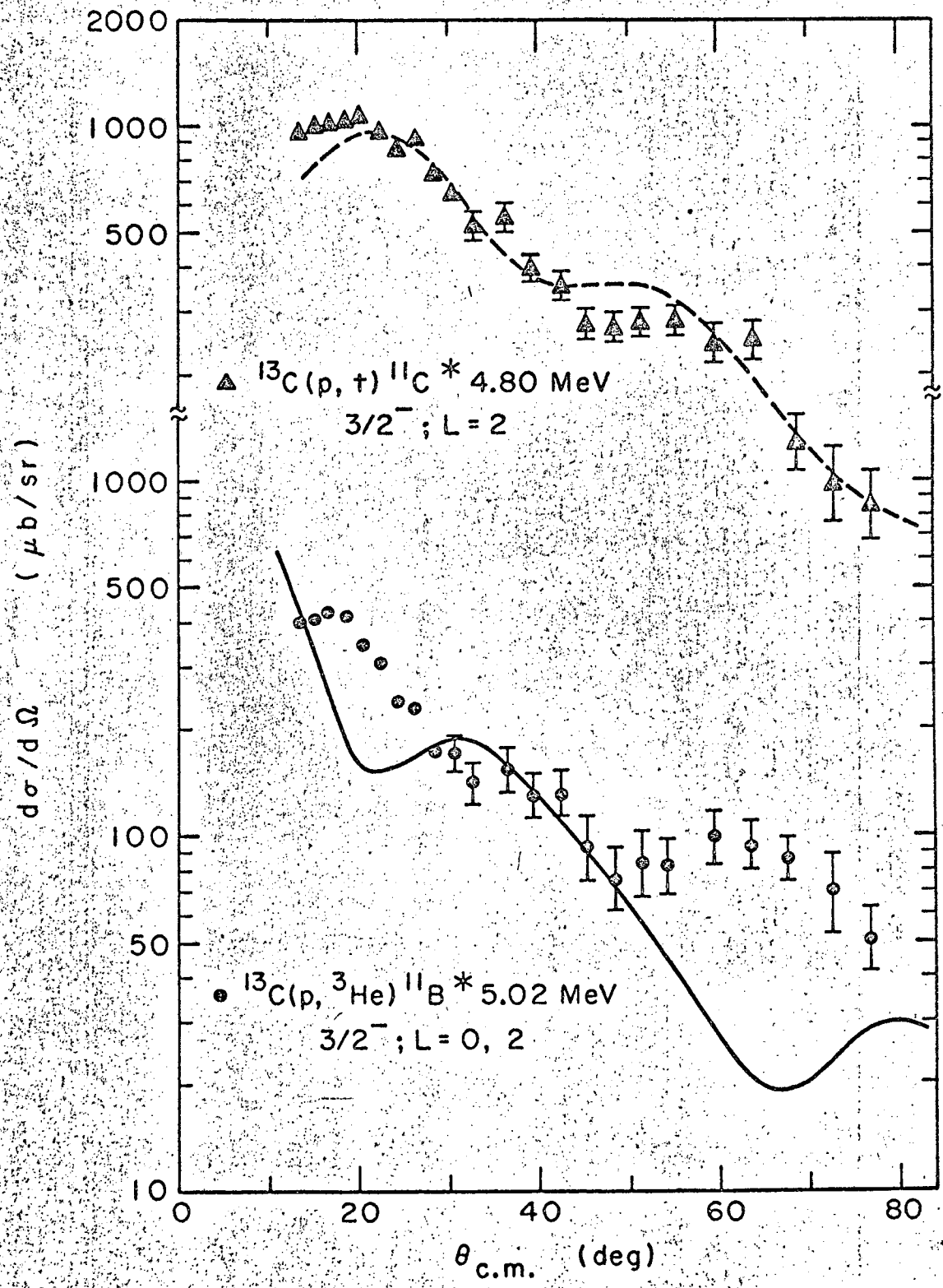
2000
1000
500
1000
500
100
50
10
0
20
40
60
80
dσ/dΩ (μb/sr)
θ c.m. (deg)
▲ 13C(p, t) 11C * 4.80 MeV
3/2⁻ ; L = 2
● 13C(p, 3He) 11B * 5.02 MeV
3/2⁻ ; L = 0, 2
XBL674-2966-B

Fig. 11

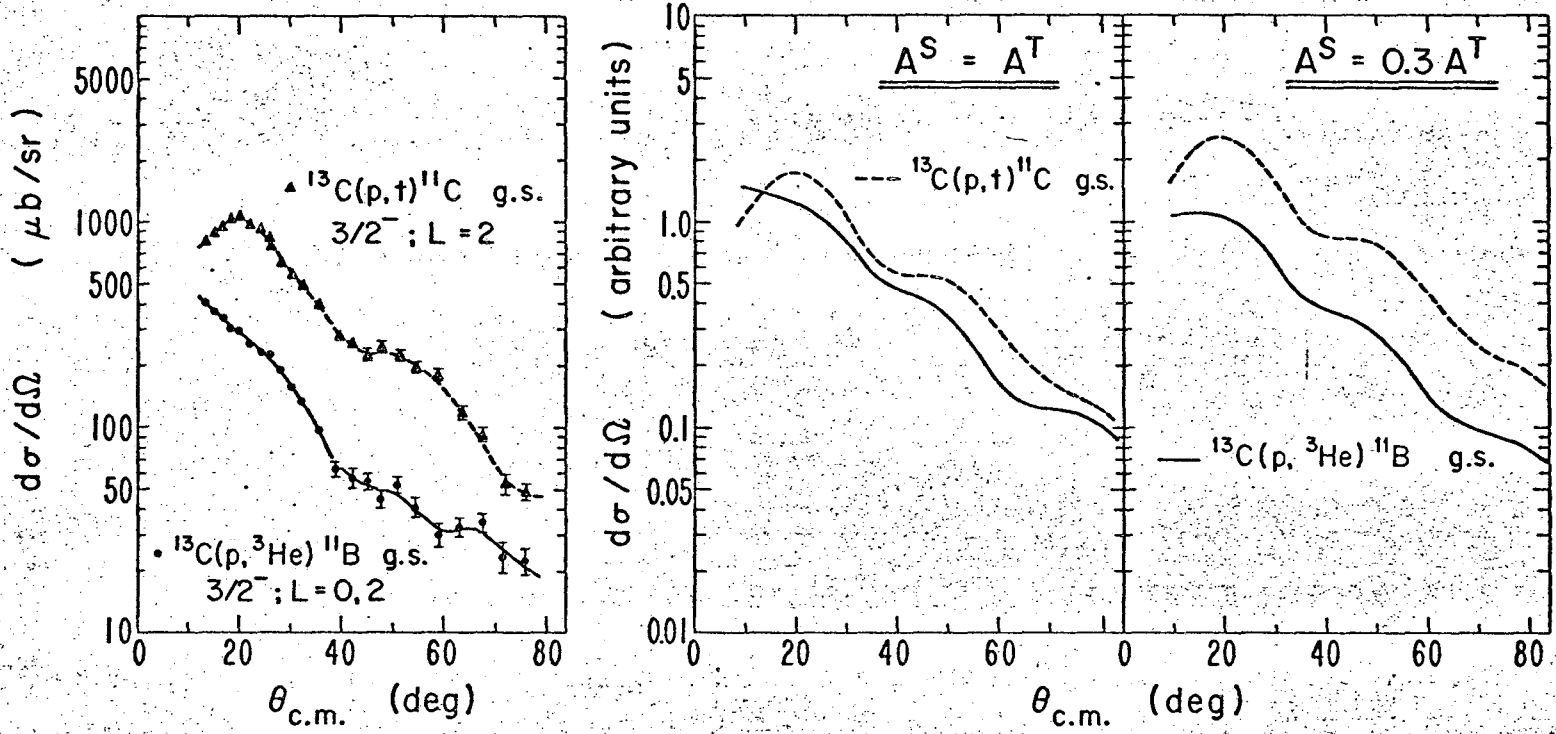
5000
1000
500
100
50
10
dσ/dΩ (μb/sr)
▲ 13C(p,t)11C g.s.
3/2⁻ ; L = 2
• 13C(p,3He) 11B g.s.
3/2⁻ ; L = 0,2
0
20
40
60
80
θc.m. (deg)
10
5
1.0
0.5
0.1
0.05
0.01
dσ/dΩ (arbitrary units)
AS = AT
AS = 0.3 AT
--- 13C(p,t)11C g.s.
— 13C(p, 3He) 11B g.s.
0
20
40
60
80
θc.m. (deg)
XBL674-2973-A

Fig. 12

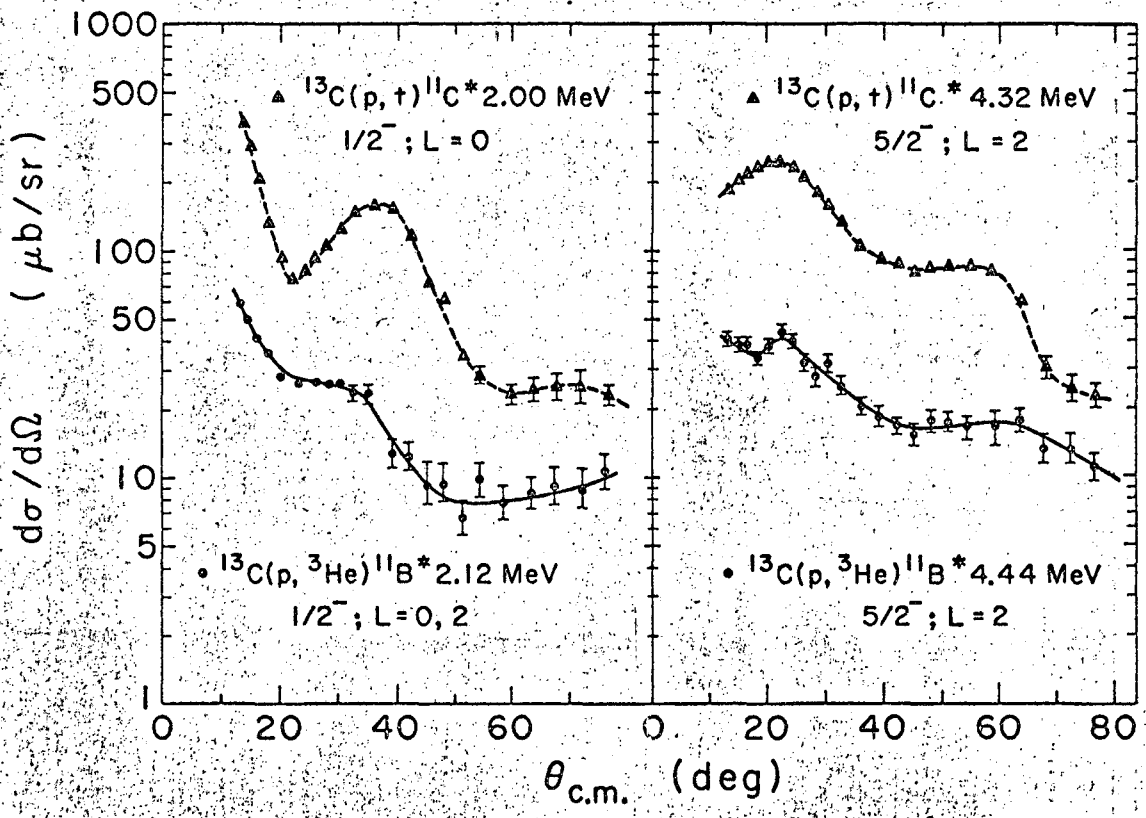
1000
500
100
50
10
5
1
dσ/dΩ (μb/sr)
▲ 13C(p, t)11C*2.00 MeV
1/2⁻; L = 0
▲ 13C(p, t)11C*4.32 MeV
5/2⁻; L = 2
• 13C(p, 3He)11B*2.12 MeV
1/2⁻; L=0, 2
• 13C(p, 3He)11B*4.44 MeV
5/2⁻; L = 2
0 20 40 60
0 20 40 60 80
θc.m. (deg)
XBL674-2971

Fig. 13

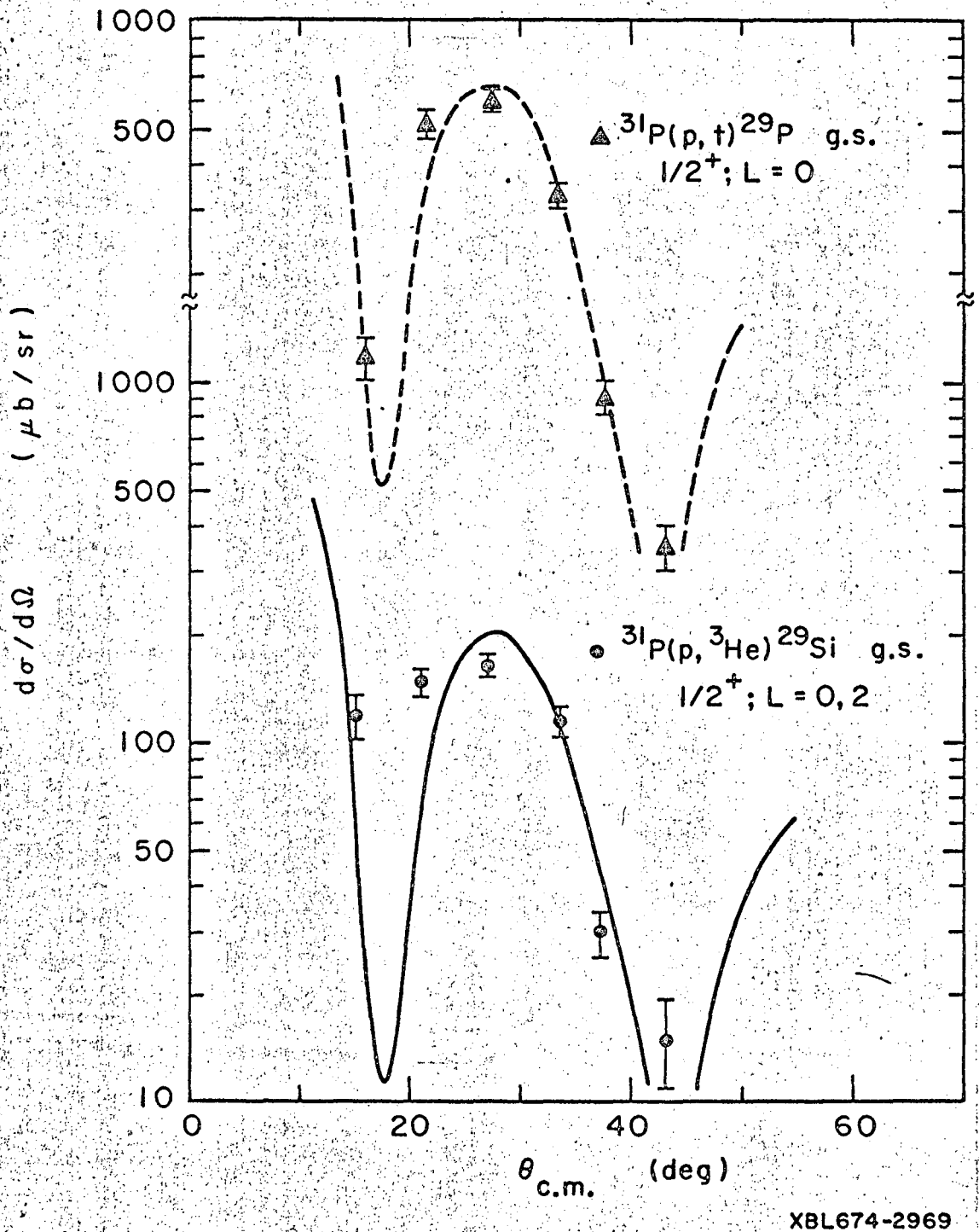
1000
500
1000
500
100
50
10
0
20
40
60
$^{31}P(p,t)^{29}P$ g.s.
$1/2^+$; L = 0
$^{31}P(p,^3He)^{29}Si$ g.s.
$1/2^+$; L = 0, 2
$d\sigma/d\Omega$ ($\mu b/sr$)
$\theta_{c.m.}$ (deg)
XBL674-2969

Fig. 14

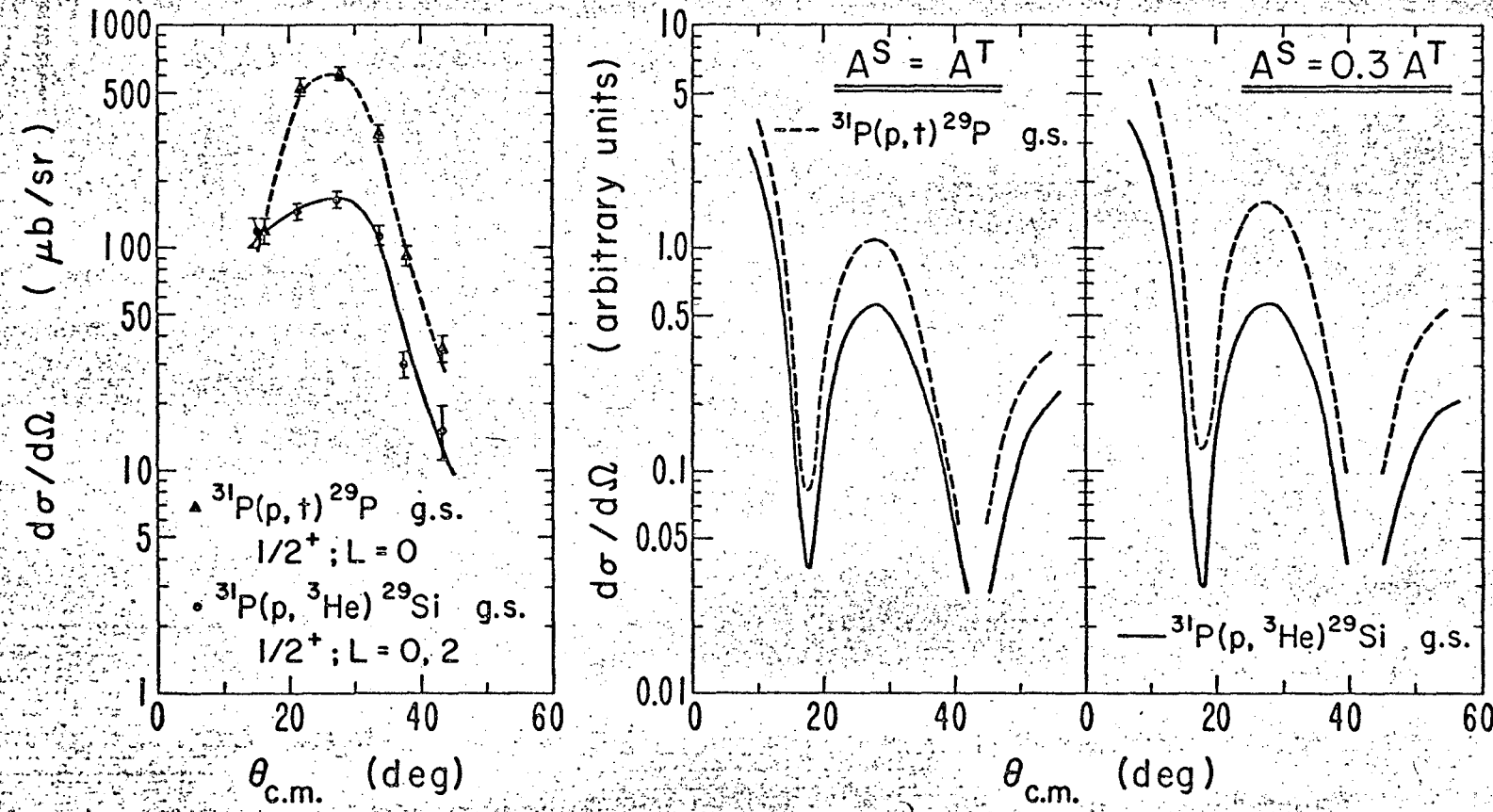
1000
500
100
50
10
5
1
dσ/dΩ (μb/sr)
▲ 31P(p, t) 29P g.s.
1/2+ ; L = 0
• 31P(p, 3He) 29Si g.s.
1/2+ ; L = 0, 2
0
20
40
60
θc.m. (deg)
10
5
1.0
0.5
0.1
0.05
0.01
dσ/dΩ (arbitrary units)
AS = AT
--- 31P(p,t)29P g.s.
AS = 0.3 AT
— 31P(p, 3He)29Si g.s.
0
20
40
0
20
40
60
θc.m. (deg)
XBL674-2974-A

Fig. 15

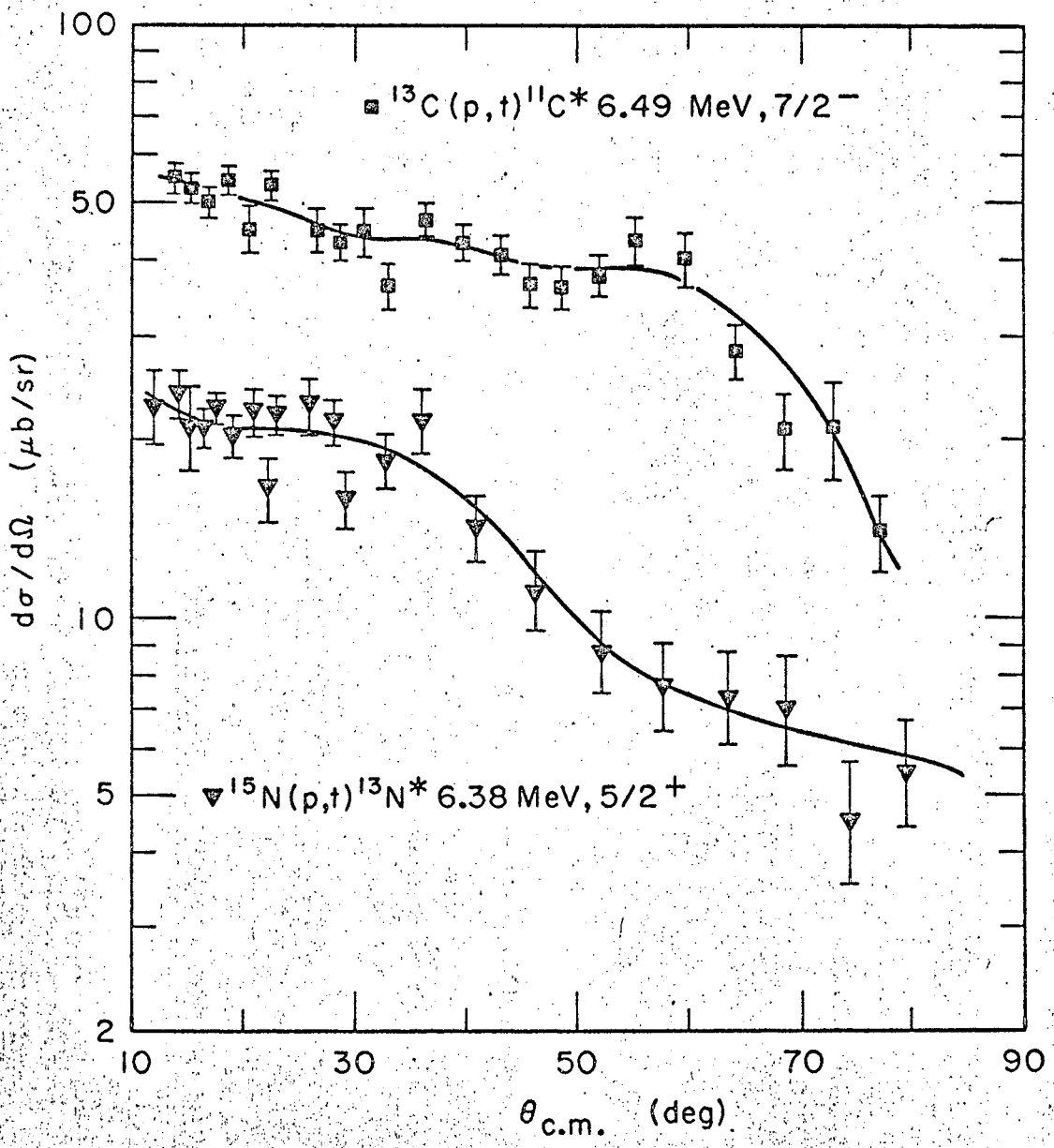

XBL676-3267

Fig. 16

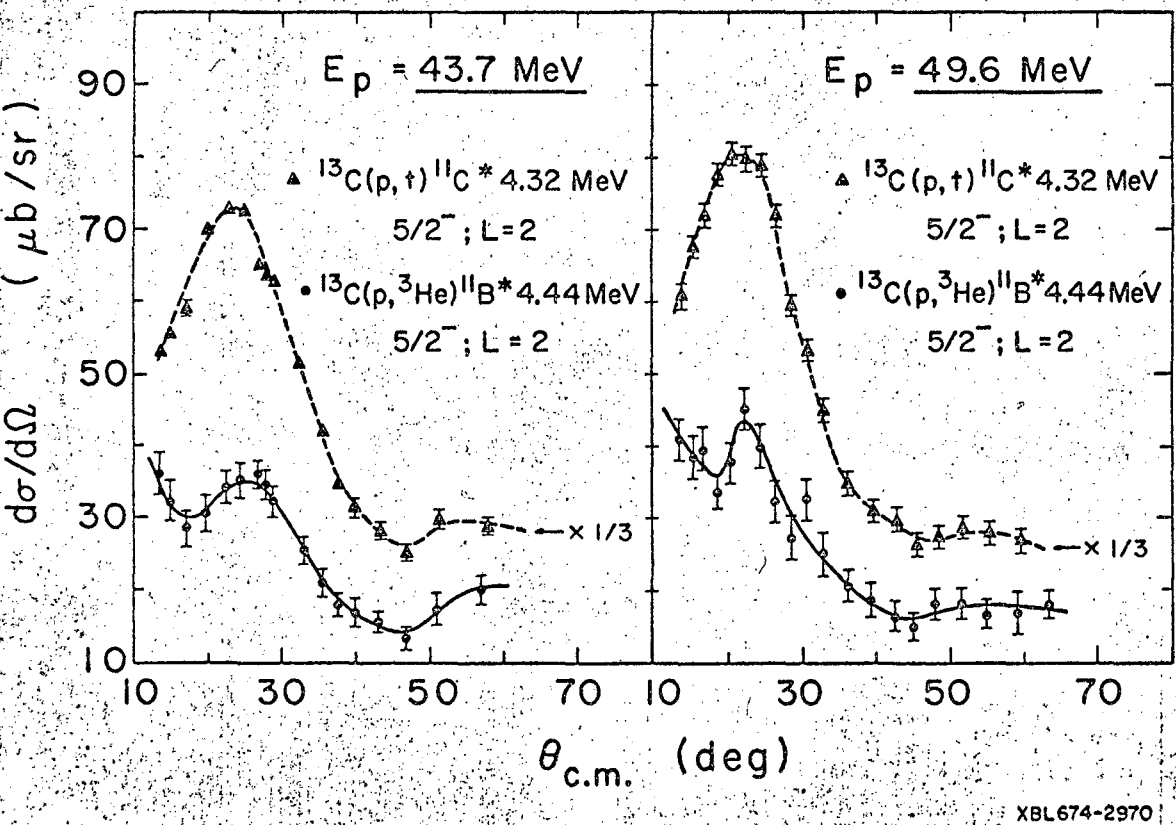
E_p = 43.7 MeV
E_p = 49.6 MeV
▲ $^{13}C(p,t)^{11}C^*$ 4.32 MeV
5/2⁻; L=2
● $^{13}C(p,^3He)^{11}B^*$ 4.44 MeV
5/2⁻; L=2
× 1/3
dσ/dΩ (μb/sr)
90
70
50
30
10
10
30
50
70
$\theta_{c.m.}$ (deg)
XBL674-2970

Fig. 17